

SSRMP Annual Scientific Meeting 2012

Kongresshaus Biel 15th and 16th of November 2012



Proceedings & Abstracts

ISBN 3 908 125 53 7

Available on www.sgsmp.ch and CD

Editors: M.K. Fix and P. Manser

Schweizerische Gesellschaft für Strahlenbiologie und Medizinische Physik
Société Suisse de Radiobiologie et de Physique Médicale
Società Svizzera di Radiobiologia e di Fisica Medica
Swiss Society of Radiobiology and Medical Physics

SGSMP
SSRPM
SSRFM

Dear colleagues and friends

The Annual Scientific Meeting 2012 of the Swiss Society of Radiobiology and Medical Physics took place in Biel on the 15th and 16th of November 2012. It was a great pleasure to welcome so many colleagues and friends from Switzerland and abroad.

The scientific program of the annual meeting was structured into six sessions with four invited speakers who addressed topics of current interest in radiation therapy and beyond. To honor the memory of Dr. Roberto Mini and to provide a new platform for young researchers, a special session was added to this year's regular scientific program: the Mini-Symposium. The aim of this session was to give PhD or MSc students the possibility to present their work, either ongoing or finished, and to share their research ideas with us. We were very pleased to see that our young colleagues appreciated this opportunity and we could enjoy presentations at a remarkable high level. With this in mind we can be certain that research in our field will continue to be the basis of our daily clinical work guaranteeing a high standard of quality.

Our annual meeting cannot be organized on a high level without the generous support of our industrial partners and we would like to thank them for their participation and continuous support. In addition, we want to thank all the other people that contributed to the success of the meeting, in particular our colleagues for their scientific contributions.

On behalf of the local organizing committee

Daniel Vetterli

Radio-Onkologiezentrum Biel-Seeland–Berner Jura
Centre de radio-oncologie Bienne-Seeland–Jura bernois



 **INSELSPITAL**
UNIVERSITÄTSSPITAL BERN
HOPITAL UNIVERSITAIRE DE BERNE
BERN UNIVERSITY HOSPITAL

The Annual Scientific Meeting of the Swiss Society of Radiobiology and Medical Physics (SSRMP) was jointly organized by the Radio-Onkologiezentrum Biel and the Division of Medical Radiation Physics of InselSpital – University Hospital Bern.

Congress president

Daniel Vetterli

Local organizing committee

Chair: Daniel Vetterli

Members: Pascal Favre-Bulle, Michael Fix, Peter Manser,
Dario Terribilini

Scientific committee

Chair: Pascal Favre-Bulle

Members: Giovanna Dipasquale, Antonella Fogliata,
Stephan Klöck, Peter Manser, Regina Seiler,
Francis Verdun

Main Program

- 09:00 – 10:00** **Registration and Coffee**
- 10:00 – 10:15** **Opening ceremony**
D. Vetterli, Congress president
R. Moeckli, President SSRMP
- 10:15 – 12:15** **Session 1: Treatment Planning**
Chairpersons: R. Seiler and S. Bulling
-

- 10:15 (O01) **Experiences with the new CMS Xio IMRT Smart-Sequencer**
Yasar Avcu, Nicolas Hanauer, Götz Kohler
- 10:30 (O02) **Reducing operator bias in IMRT optimization / Experience-based optimization**
Grégory Bolard, Nasser Hejira, Shelley Bulling
- 10:45 (O03) **Small static and RapidArc fields generated by MLC only: MU calculation accuracy for AAA and Acuros XB.**
Alessandro Clivio, Antonella Fogliata, Giorgia Nicolini, Eugenio Vanetti, Luca Cozzi
- 11:00 (O04) **Dosimetric evaluation of different treatment techniques for breast cancer with simultaneous integrated boost.**
Shaun Graydon, Stephanie Lang, Sarah Verlaan, Michelle Malla, Mariangela Zamburlini, Anja Stüssi, Christoph Glanzmann and Stephan Klöck
- 11:15 (O05) **Clinical impact of Acuros XB dose calculation algorithms in cases with lung or bone involvement**
Giorgia Nicolini, Alessandro Clivio, Antonella Fogliata, Eugenio Vanetti, Luca Cozzi
Oncology Institute of Southern Switzerland, Bellinzona, Switzerland
- 11:30 (O06) **Commissioning and implementation of a commercial Monte Carlo based treatment planning system**
V. Magaddino, O. Pisaturo, M. Pachoud, V. Vallet, S. Thengumpallil, F. Bochud, R. Moeckli
- 11:45 (IS01) **Invited Speaker: U. Oelfke, DKFZ, Heidelberg, Germany**
Uncertainties in Hadron Therapy: Challenges and Potential Solutions

Main Program

- 12:15 – 12:45** *Poster viewing and industrial exhibition*
Lunch break
- 12:45 – 13:45** *Lunch Symposium*
- 13:45 – 15:00** *Session 2: Navigation and Brachytherapy*
Chairpersons: P. Pемler and D. Terribilini
-

- 13:45 (IS02) **Invited Speaker: S. Weber**, ARTORG, University of Bern, Switzerland
Novel Perspectives in Image Guidance Interventions
- 14:15 (O07) **First Clinical Experience with IORT of Breast Cancer using soft X-Rays of Intrabeam® by Carl Zeiss**
Binder Jörg, Damoune Hans, Madry-Gevecke Britta, Breitbach Petra
- 14:30 (O08) **Surface dose optimization of the Varian Ir-192 HDR surface applicator set with vertical Leipzig-style cone**
Konrad Buchauer, Hans Schiefer, Ludwig Plasswilm
- 14:45 (O09) **Validation and evaluation of a collapsed cone dose calculation algorithm for HDR brachytherapy**
Dario Terribilini, Werner Volken, Michael K. Fix, Kristina Lössl, Peter Manser
- 15:00 – 15:30** *Poster viewing and industrial exhibition*
Coffee break
- 15:30 – 16:30** *Session 3: Quality Assurance*
Chairpersons: P. Favre-Bulle and S. Klöck
-

- 15:30 (O10) **In-vivo thermoluminescent dosimetry assessment of target dose delivery using IMRT and VMAT in patients with ano-rectal cancer**
Dipasquale G, Nouet P, Rouzaud M, Dubouloz A, Sedmak C, Miralbell R, Zilli T
- 15:45 (O11) **Definition of Parameters for Quality Assurance of Flattening Filter Free (FFF) Photon Beams in Radiation Therapy**
Antonella Fogliata, Alessandro Clivio, Giorgia Nicolini, Eugenio Vanetti, Luca Cozzi
- 16:00 (O12) **Weekly QA of linac dosimetry using a 2-D detector array**
Natacha Ruiz Lopez, J.-F. Germond, R. Moeckli
-

Main Program

- 16:15 (O13) **Results from testing the Octavius pre-treatment QA system equipped with the inclinometer**
Eugenio Vanetti, Alessandro Clivio, Antonella Fogliata, Giorgia Nicolini, Luca Cozzi
- 16:30 – 18:00** *SSRMP General Assembly*
- 18:15 – 18:45** *Transfer to Römerhof*
- 18:45** *Conference Dinner at Römerhof*

Main Program

08:30 – 10:15 **Session 4: Advanced Techniques**
Chairpersons: M.K. Fix and G. Dipasquale

- 08:30 (IS02) **Invited Speaker: J. Cygler**, The Ottawa Hospital Cancer Centre, Ottawa, Canada
Clinical electron beams in the era of commercial Monte Carlo based treatment planning systems
- 09:00 (O14) **Dosimetric properties of an amorphous silicon EPID for verification of modulated electron radiotherapy**
Cécile Chatelain, Daniel Vetterli, Daniel Morf, Dominik Henzen, Pascal Favre, Michael K. Fix, Peter Manser
- 09:15 (O15) **Physical Aspects of Total Skin Electron Irradiation at the University Hospital Basel**
Götz Kohler, Roman Menz, Renate Nyffenegger, Frank Zimmermann
- 09:30 (O16) **Interplay effect between respiratory motion and dynamic irradiation: Experimental test of a simple analytical model**
J.-F. Germond, S. Thengumpallil, R. Moeckli
- 09:45 (O17) **Investigation of the dose accuracy and benefits of gated IMRT and VMAT for clinical implementation**
Angèle Dubouloz, Coline Corbet, Dolores Leduc
- 10:00 (O18) **First tests with a new 6 degrees of freedom couch**
Daniel Schmidhalter, Michael K. Fix, Marcel Wys, Niklaus Schaer, Peter Munro, Stefan Scheib, Martin Amstutz, Peter Manser

10:15 – 10:45 **Poster viewing and industrial exhibition**
Coffee break

10:45 – 12:30 **Session 5: MINI Symposium**
Chairpersons: P. Manser and R. Moeckli

- 10:45 (M01) **Evaluation of the 'worst case scenario' approach to handle setup uncertainties in proton treatments**
Margherita Casiraghi, Francesca Albertini, Antony John Lomax
- 10:57 (M02) **Monitor units are not predictive of neutron dose for high-energy IMRT**
Roger A. Hälgl, Jürgen Besserer, Markus Boschung, Sabine Mayer, Uwe Schneider

Main Program

- 11:09 (M03) **Measurements of whole-body dose distributions in radiotherapy for different treatment machines and delivery techniques**
Roger A. Halg, Jurgen Besserer, Uwe Schneider
- 11:21 (M04) **Direct aperture optimization concept for inverse planning of modulated electron radiotherapy**
Dominik Henzen, Peter Manser, Daniel Frei, Werner Volken, Hans Neuenschwander, Ernst J. Born, Michael K. Fix
- 11:33 (M05) **Eye-Tracking human observers in lung CT volumetric detection tasks**
Ivan Diaz, Sabine Kobbe-Schmidt, Francis R. Verdun, Franois O. Bochud
- 11:45 (M06) **Combining wave-optics and Monte Carlo methods for the simulation of grating based hard X-ray interferometry**
Silvia Peter, Peter Modregger, Michael K Fix, Werner Volken, Peter Manser, Marco Stampanoni
- 11:57 (M07) **Respiratory-correlated cone beam CT as a pre-treatment tool for free breathing lung treatment: a phantom study**
S.Thengumpallil, J-F. Germond, J. Bourhis, F.Bochud, R. Moeckli
- 12:09 (M08) **Portal Dosimetry verification for VMAT: a comparative study of two methods**
Paolo Zucchetti
- 12:30 – 14:00** *Poster viewing and industrial exhibition*
Lunch break
- 14:00 – 16:00** *Session 6: Diagnostic Imaging*
Chairpersons: F. Corminboeuf and H. Roser
-
- 14:00 (IS04) **Invited Speaker: M. Stampanoni**, ETH Zurich and PSI Villigen, Switzerland
Sensing the phase: a breakthrough for (bio)medical imaging?
- 14:30 (O19) **Implementation of a Monte Carlo model for dose calculations in small animal imaging at TOMCAT beamline**
Silvia Peter, Goran Lovric, Michael K Fix, Werner Volken, Daniel Frei, Peter Manser, Marco Stampanoni

Main Program

14:45 (O20) **Assessment of the exposure of the Swiss population to computed tomography**
Abbas Aroua, François O Bochud, Reto Meuli, Barbara Ott, Elina Samara, Reto Treier, Philippe P Trueb, Francis R Verdun

15:00 (O21) **Clinical Audits in RADIOLOGIE in Switzerland**
Carine Galli Marxer, Reto Treier, Philipp R. Trueb

15:15 (O22) **Image quality characterisation of time-of-flight and point-spread-function corrections in the PET/CT Discovery-690**
S. Gnesin, J. Delacoste, P. Martinez, M. Pappon, J.O. Prior, F. Verdun,

15:30 (O23) **Involvement of medical physicists in diagnostic radiology and nuclear medicine**
Treier Reto, Zeller Werner, Trueb Philipp R.

15:45 (O24) **Diagnostic Reference Levels in Nuclear Medicine – an Update for Switzerland**
Hans W. Roser

16:00 **Closing**

Main Program: Posters

List of Poster presentations

- (P01) **Dose Distribution Analysis of Small Fields in Electron Beam Therapy using Radiochromic Films**
L. De Abreu Vieira, G. Kohler
- (P02) **Case report: IMRT plan verification in homemade phantoms for Ewing sarcoma treatment around a distant femoral implant.**
Dipasquale Giovanna, Dubouloz Angèle, Nouet Philippe
- (P03) **Implementation of ISP Gafchromic EBT3 film using commercial software**
Angèle Dubouloz
- (P04) **Radiation Transport Through Beam Modifiers for Proton Radiotherapy Using Macro Monte Carlo**
M. K. Fix, D. Frei, W. Volken, E.J. Born, D.M. Aebersold, P. Manser
- (P05) **Linac Radiation Shielding under clinical conditions - Radiation Protection Case Report**
Käthy Haller, Stephan Scheidegger, Gerd Lutters
- (P06) **Evaluation of the RADPAD® Scatter Protection Shielding using an Alderson phantom in a clinical situation (cardiology)**
Käthy Haller, Barbara Markert, Leandro De Abreu Vieira, Gerd Lutters, Stephan Scheidegger
- (P07) **Comparison of VMAT plans with variable and constant dose rate and gantry speed for pelvic cancer treatment**
Nasser Hejira, Grégory Bolard, Shelley Bulling
- (P08) **Film dosimetry with ImageMagick**
Götz Kohler, Leandro De Abreu Vieira
- (P09) **Penetration depth of heat produced by superficial hyperthermia applicator in a muscle equivalent phantom material at different surface cooling temperatures**
Dietmar Marder
- (P10) **Development of Scatter Correction Methods for Micro Cone Beam Computed Tomography**
W. Volken, M. K. Fix, D. Frei, M. A. Zulliger, P. Manser

(P11)

Qualitative assessment of radiation protection behavior of interventional radiology/cardiology staff using active dosimetry

Nick Ryckx, Francis R. Verdun, Marta Sans-Merce, Jean-Christophe Stauffer, Alban Denys, Yann Lachenal, Olivier Muller

O01

Experiences with the new CMS Xio IMRT Smart-Sequencer

Yasar Aycu, Nicolas Hanauer, Götz Kohler

Klinik für Strahlentherapie und Radioonkologie, Universitätsspital Basel, Switzerland

With the CMS Xio release 6.62.05 a new sequencer (*Smart Sequencer*) for the step and shoot IMRT was provided in the radio therapy planning system. With this new sequencer, the number of segments and number of total monitor units (MU) decreases, whereas the quality of the dose distribution remains unchanged.

In the present work, the differences between the hitherto available sequencer *Sliding-Window* and the current sequencer *Smart-Sequencer* are discussed. Furthermore, a plan comparison is presented, that is based on seven retrospective prostate IMRT plans, which were originally planned using the *Sliding-Window* sequencer. These plans were now repeated based on the new sequencer with the same dose-prescription of 64 Gy in the Planning Target Volume (PTV) and which were calculated respectively under identical dose restrictions with each of the segmentation algorithms.

At the subsequent analysis, the quality of the dose distribution in the PTV, the number of segments, the number of total MUs, as well as the dose of the rectum- and bladder wall were compared.

The segmentation with the *Smart-Sequencer* implicates that the number of segments decreases for each plan (on average 72% less) and that the total number of irradiated MUs is reduced for each plan (on average 28% less). For this reason, the treatment period considerably declines, whereas the covering of the target volume partly improves and the stress on the risk organs stays alike.

However, despite all advantages, there is one minus: computing time with the *Smart Sequencer* is larger, because this method additionally requires a Segment-Weight-Optimization in which the individual weights of the segments are optimized (not only the weights of the beams). At the moment, our institution uses the new sequencer for almost all IMRT plans with exception of the head and neck region.

O02

Reducing operator bias in IMRT optimization / Experience-based optimization

Grégory Bolard(1), Nasser Hejira(1), Shelley Bulling(2)

(1) Clinique de Genolier, Genolier, Switzerland

(2) Centre d'oncologie des Eaux-Vives, Genève, Switzerland

Although a lot of tools are available in modern treatment planning systems to evaluate a 3D dose distribution (DVH, biological indices, isodoses in arbitrary planes), the optimality of a given IMRT/VMAT plan still depends mainly on the experience of the planner for the relevant clinical site, and on the way that the optimization problem has been formulated in terms of dose objectives. To overcome this bias, we decided to use our experience in IMRT optimization to predict dose objectives based on individual patient geometry prior to optimization. In this study we focused on prostate cancer. We reviewed all photon IMRT/VMAT plans treated in the past two years and found that the final equivalent uniform dose (EUD) for bladder and rectum showed a strong correlation with the overlap volume with the PTV. Therefore, plans with non-favourable patient geometry are classified as non optimal for bladder and rectum sparing. Based on their respective overlap volume, we used these relationships to predict objectives for rectum and bladder (EUD). These actions were implemented by user scripting in our treatment planning system (Philips Pinnacle³). The implementation of this experience-based IMRT has shortened the treatment planning time and reduced the operator bias on achieving good quality IMRT & VMAT plans. We plan to extend this approach to other standardized clinical sites.

O03

Small static and RapidArc fields generated by MLC only: MU calculation accuracy for AAA and Acuros XB.

*Alessandro Clivio, Antonella Fogliata, Giorgia Nicolini, Eugenio Vanetti, Luca Cozzi
Oncology Institute of Southern Switzerland, Bellinzona, Switzerland*

Purpose: to evaluate the accuracy in MU calculation of AAA and Acuros XB photon dose calculation algorithms implemented in Eclipse treatment planning systems, in cases where small fields are generated by MLC setting, while rather broad jaw setting is defined.

Materials and Methods: Output from small fields (0.6x1, 1x1, 2x2, 3x3 cm²) set with MLC keeping 12x12 cm² jaw setting were measured in water phantom with a natural diamond detector (PTW). A 6 MV beam from a Varian Clinac iX equipped with a 120 leaves MLC was used. Measurements were compared to calculations from the Varian Eclipse planning system using two dose calculation algorithms: the Anisotropic Analytical Algorithm AAA and Acuros XB. The wide jaw setting selection was imposed in order to evaluate the MU calculation in conditions where the collimator backscatter factor does not force the MU calculation in the case of small apertures, and the MU calculation is therefore driven by the algorithm itself.

MU calculation has been evaluated also changing the configuration parameter of focal spot size, MLC transmission and MLC dosimetric leaf gap.

Two RapidArc plans were prepared with the same jaw setting of 12x12 cm², optimizing to deliver homogeneous dose to the anterior part of a ring of 3 (4) cm thickness, shielding the central part of 4 (2) cm diameter (with a margin of 0.5 cm between target and central shielded volume). The total arc length was 220 degree, collimator rotation 90 degree. Doses were measured in the central part (always shielded) and in the middle of the virtual target ring (almost always open) with a 0.125 cm³ ion chamber (semiflex, PTW) and compared with Acuros XB calculations.

Results: Small field output showed a difference of maximum +2% for Acuros calculations with respect to measurements for all analyzed fields; larger deviation for 1x1 and 0.6x1 cm² fields (-2.8 and -4.6%, respectively) were found for AAA calculations; for smaller fields Acuros showed a dose overestimation, while AAA a dose underestimation.

RapidArc plans (Acuros XB only) presented an average dose difference (with respect to the mean dose to the target) in the target ring of -1.3% and -0.4% respectively for the two RapidArc plans, and of -4.5 and -1.4% respectively in the central shielded point.

Conclusion: AAA and especially Acuros XB were found to accurately calculate MU in small MLC defined fields.

O04

Dosimetric evaluation of different treatment techniques for breast cancer with simultaneous integrated boost.

Shaun Graydon, Stephanie Lang, Sarah Verlaan, Michelle Malla, Mariangela Zamburlini, Anja Stüssi, Christoph Glanzmann and Stephan Klöck
Department of Radiation Oncology, University Hospital, Zurich, Switzerland

Objective

Dosimetrical comparison of volumetric arc therapy (VMAT), intensity modulated radiation therapy (IMRT), electronic compensation (EC) and 3D conformal (3D) techniques for hypofractionated breast radiotherapy with simultaneous integrated boost (SIB). Finally the evaluation of the robustness of these techniques under breathing conditions.

Materials and Methods

Five patients were selected of varying breast size (276 cc, 630 cc 955 cc, 1012 cc and 1339.8cc). Four dosimetrists were randomly assigned a technique, either VMAT, IMRT, EC or 3D. Each of them created a plan for each patient with the assigned technique. Thus each patient was planned 4 times. Plans were optimized to meet the criteria from the Radiation Therapy Oncology Group (RTOG) trial - 1005. Quality assurance for plan robustness was performed using a Delta4 phantom on a moving couch top. A breathing amplitude of 1cm and a breath frequency of once every 5 seconds was used. A gamma score (2mm/3%) of 95% was considered acceptable. To evaluate the changes in dose to organs at risk together with company CIRS a realistic anthropomorphic breast phantom was designed, which allows Gafchromic film measurements in each slice of the phantom. The aim is to quantify on a high resolution detector system the interplay effects between the dynamics of dose delivery and patient motion.

Results

PTV coverage was comparable for all techniques. All plans achieved RTOG-1005 objectives. VMAT delivered significantly more dose to the contra-lateral breast ($p > 0.01$) and the contra-lateral lung ($p > 0.01$) compared to all other techniques. Treatment times were compared for the four techniques, VMAT was the fastest (151 s) whereas EC took the most time to deliver (236 s). Gamma scores for the static phantom control measurement were equally good (VMAT 98.82% +/-1.16%, IMRT 99.81% +/-0.58%, 3D 98.16% +/-4.96% and EC 98.84% +/-2.55%). RA was most robust against motion (VMAT 95.40% +/-4.57%, IMRT 93.62% +/-8.89%, 3D 91.32% +/-16.48% and EC 84.45% +/-17.37%). For IMRT, 3D and EC treatment fields with less than 40 MU were most sensitive to breathing motion. A decrease in dose rate for these fields from 400 MU/min to 100 MU/min, significantly improved the gamma score for these fields (e.g. EC from 61.8 % to 84.0 %).

Conclusion

All plans have their merits and disadvantages. Further investigations are planned to evaluate the dose at the air-tissue interface as well as doses to organs at risk under motion using Gafchromic films in mentioned modified anthropomorphic phantom. Fields with a low number of monitor units and high modulation should be avoided as they can result in low gamma scores depending on phase of breathing cycle. Lowering the dose rate from 600 MU/min to 100 MU/min improved these gamma scores.

O05

Clinical impact of Acuros XB dose calculation algorithms in cases with lung or bone involvement

*Giorgia Nicolini, Alessandro Clivio, Antonella Fogliata, Eugenio Vanetti, Luca Cozzi
Oncology Institute of Southern Switzerland, Bellinzona, Switzerland*

Purpose: Acuros[®] XB is a photon dose calculation algorithm implemented in the Varian Eclipse TPS. In particular Acuros XB allows the dose to medium calculation, accounting for the supposed chemical composition of the human body, through CT range to tissue correspondences. The study aims to assess the impact of this algorithm in clinical cases, in particular where low density medium as lung, or high density as bone are involved in the treatment, using volumetric modulated arc therapy in the RapidArc form.

Methods and Materials: For low density medium analysis, CT dataset of ten patients presenting advanced NSCLC were selected and contoured for PTV, lungs, heart, spinal cord. Dose was prescribed to 66 Gy in 33 fractions to mean planning target volume (PTV). For high density medium analysis, CT dataset of ten patients presenting soft tissue sarcoma of the leg surrounding the femur were selected and contoured for PTV and bone. Dose was prescribed to 66.5 Gy in 25 fractions to mean PTV, and significant maximum dose to the bone was limited to 50 Gy.

All plans were prepared using RapidArc technology for a 6MV beam. Calculations were performed with Acuros XB and AAA (Anisotropic Analytical Algorithm) with the same MU, the former in its two options of dose to medium and dose to water for the cases with bone involvement.

Results: *NSCLC and lung tissue:* percentage difference, with respect to the structure mean dose, between AAA and Acuros XB calculations were analyzed, averaged over all 10 patients. PTV dose difference was stratified between the target in soft and lung tissue, presenting mean dose difference of $+1.4\pm 0.2\%$ and $-0.2\pm 0.2\%$ respectively. Mean doses to OARs presented mean differences between $-0.5\pm 0.2\%$ (contralateral lung) to $0.9\pm 0.2\%$ (heart).

Sarcoma and bone tissue: mean dose differences between AAA and Acuros XB to medium and to water were, respectively, $+1.8\pm 0.3\%$ and $+1.4\pm 0.6\%$. Mean differences for the significant maximum dose in the bone were $-4.0\pm 0.8\%$ for dose to medium calculation, and $+9.2\pm 1.1\%$ for dose to water.

Conclusion: the availability of Acuros XB could improve the patient dose estimation, that could be clinically significant in particular cases where inhomogeneities play a critical role as lung and bone tissues. Correlations between more accurate dose calculations and clinical data are today advisable.

O06

Commissioning and implementation of a commercial Monte Carlo based treatment planning system

V. Magaddino(1), O. Pisaturo(2), M. Pachoud(1), V. Vallet(1), S. Thengumpallil(1), F. Bochud(1), R. Moeckli(1)

(1) Institute of Radiation Physics, Lausanne University Hospital, Lausanne

(2) Service de Radio-oncologie, Hôpital Cantonal de Fribourg, Fribourg

Fast and accurate Monte Carlo (MC) based treatment planning systems (TPS) have become commercially available. The aim of this study is the dosimetric validation of the MC based TPS Monaco (CMS Elekta, version 3.1) and the clinical implementation of VMAT and IMRT techniques.

Dose distributions calculated with Monaco have been compared to measurements in water and solid water phantom performed with both ionization chambers and a 2D detector array. The Monte Carlo algorithm implemented in Monaco is based on the XVMC code, and a virtual energy source model is used to describe the treatment head. The voxel size used for the MC calculated dose distributions was 2mm with a statistical uncertainty <0.5%. Static on-axis and off-axis fields were studied for a 6MV photon beam. Simulated percent depth doses, profiles, and output factors have been compared with the corresponding measurements. An experimental setup consisting of several heterogeneous slabs of different material densities was also used to investigate the dosimetric accuracy of the calculation in heterogeneous media. Additionally, IMRT and VMAT patient plans were optimized using the biological cost function for target and organs at risk, and the calculated dose distributions were compared with measurements performed in the Delta4 phantom.

MC simulations for static fields are in good agreement for the different configuration and setup used in the study. An overall agreement of 2%/2 mm between simulation and measurement with ionization chamber and 2D array measurements was found in all cases. Comparisons of calculated and measured dose distribution for dynamic cases (IMRT and VMAT) also showed a good agreement (better than 3%/3mm).

These results allowed us to validate Monaco MC based TPS for its use in clinical practice.

O07

First Clinical Experience with IORT of Breast Cancer using soft X-Rays of Intrabeam® by Carl Zeiss

*Binder Jörg, Damoune Hans, Madry-Gevecke Britta, Breitbach Petra
Kantonsspital Münsterlingen, Radiology, Switzerland*

Introduction

The Intrabeam® by Carl Zeiss, Oberkochen system offers an opportunity for treating breast cancer directly in the operation theatre (IORT). This gives rise to an immediate start of radiation therapy without delays caused by wound healing and potential chemo-therapy. So a better outcome can be expected because of fewer cell repopulation. Besides it facilitates an improved and error free localization of the tumour bed which else has to be found indirectly by means of clips etc. in the medical imaging used for the boost therapy external beam planning. Less side effects might be expected due to a reduced treated volume because no margins are needed and the X-ray source provides a spherical dose distribution with a relatively steep dose gradient, which scales as $1/r^3$ according to experimental findings. Figure 1 shows the principals of the method. A reduction of the total time of treatment from 6.5 to 4.5 - 5 weeks is possible, if IORT is given as a boost as it is the predominant case in our hospitals in Frauenfeld and Münsterlingen. In cases of early stage breast cancer and for several elderly patients even an avoidance of total breast irradiation might be possible as to be proven in TARGIT-A and E trials [1-5].

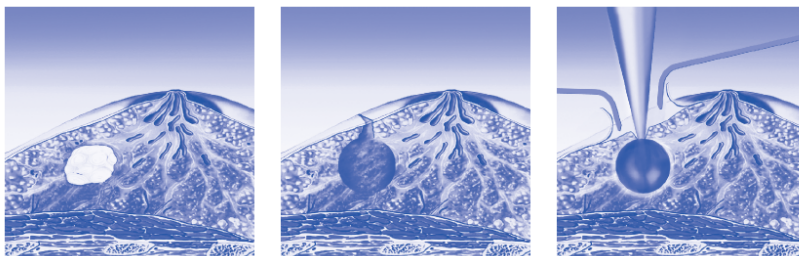


Fig. 1: Principle of Intrabeam IORT [6,7]: a) Localization of the tumour (e.g. by means of ultrasound), b) Wide operative excision of the tumour (min. resection margin 1 cm), c) Positioning of the applicator and separation of the skin to avoid wound healing complications.

The system itself consists of a fully balanced freely movable support stand, a miniature 50 kV peak X-ray source with a gold foil anode of half value thickness at the top of a transmission tube with 3 mm diameter, in which the electron beam rotates on the envelope of a cone, a set of 8 different spherical applicators with diameters ranging from 1.5 to 5 cm in steps of 0.5 cm, an independent control unit interfaced to a planning computer and a set of quality assurance tools s. a. [8]. Computer controlled assistance is given for tube alignment, isotropy control of the dose distribution and output verification by means of a soft X-ray ion chamber and a conventional therapy electrometer (PTW). Beam position and dose rate are internally monitored by IRM, an internal radiation monitor, measuring the backward emission of X-rays behind the gun by means of a scintillation crystal and thus controlling the deflection solenoids and correcting the treatment time for dose rate deviations. An inbuilt interlock system checks the correct entry of patient data and prevents unintended radiation exposure if the source is not correctly mounted to the support stand, an applicator is missing or mal-positioned and provides support for external controls such as door switches etc. The system is delivered pre commissioned by the manufacturer with a

library of source and applicator specific dose depth data measured on a 0.1 millimetre scale and entered into the planning computer. The treatment planning system manages the patient data, monitors the course of the treatment and finally generates standardised protocols.

The aim of this work is to present a simple approach to verify the correctness of the manufacturer's basic data within the clinically relevant tolerances and the reproducibility of the major dose distribution characteristics. According to the TARGIT-A trial protocol two different methods of dose prescription were acceptable in the trial: either 20 Gy at the applicator surface or 6 Gy at 1 cm tissue depth. Table 1 gives an overview of the corresponding dose values taken from the treatment planning system and the resulting deviations allowed. An inconsistency occurs when the diameter increases from 3 to 3.5 cm due to the fact that applicators smaller than 3 cm have aluminium beam hardening filters whereas the bigger ones do not. It has to be noted that very small applicators will be very rarely used because of the 1 cm resection margin constraints. So for the therapeutically relevant applicators a dose deviation of $\pm 15\%$ seems to be within the therapeutic window.

Applicator diameter [cm]	Dose [Gy] at 1.0 cm depth for a surface dose of 20 Gy	Rel. deviation to 6 Gy at 1 cm	Surface dose [Gy] for 6 Gy at 1.0 cm depth	Rel. deviation to 20 Gy at surface
1.5	3.4	- 43.3 %	35.9	+ 79.5 %
2	4.1	- 31.7 %	29.2	+ 46 %
2.5	5.2	- 13 %	23.2	+ 16 %
3	5.9	- 1.6 %	20.5	+ 2.5 %
3.5	4.8	- 20 %	24.8	+ 2.4 %
4	5.6	- 6.7 %	21.5	+ 7.5 %
4.5	6.2	+ 3.3 %	19.3	- 3.5 %
5	6.9	+ 15 %	17.4	- 13 %

Table 1: Dosimetric deviations between the two different prescription protocols of the TARGIT-A trial: 20 Gy at applicator surface or 6 Gy at 1 cm tissue depth.

An uncertainty interval in the same range results, if positioning errors of the free handedly placed applicator are taken into account. For typical applicators the dose gradient near to the applicator surface is ~ 14 Gy/cm. At the same time the doses at 0.5 cm distance to the applicator surface and in the middle of the therapeutic spherical shell of about 1 cm thickness are 9 - 10 Gy. This also results in a dosimetry error of 15 %.

At second we examine radiation protection issues related to the operation of this device in a surgical department and give comments on the clinical procedures.

Material and Methods

On account of the design characteristics the topics of major interest for commissioning Intrabeam were:

Output factors (absolute dose), correctness of dose depth curves due to treated volume effects in high dose single fraction treatment, potential anisotropies of dose distribution along polar angles caused by a lack of equilibrium between forward and backward scattering in the half layer target (adequate beam energy), isotropy of dose distribution along azimuthal angles because of errors in the centring of electron beam cone along forward axis (precision of deflection system).

Because of the very high costs of the dedicated measuring phantom distributed by Zeiss (CHF 80'000 at the time of commissioning) and taking into account the very high precision in mechanical positioning needed to measure dose depth curves accurately and in absolute dose for soft X-rays, we were looking for a practicable solution able to meet the clinical demands. Our

constraint was a tolerance interval of the physical measurements that would not enlarge the clinical tolerance by more than 1 %. According to Gaussian error propagation this is:

$$\sqrt{(15\% + 1\%)^2 - (15\%)^2} = 5.6\%.$$



Fig. 2: Experimental set up for absolute dosimetry

So for absolute dose we chose the simple PTW-4322 water phantom with source held by its own support stand inside the tank in mechanical contact with the 3 mm thick PMMA window of the tank, a PTW TN-23342 soft X-ray ionisation chamber outside the thin window in a chamber holder taken from PTW Soft X-ray Slab Phantom and 5 cm PMMA as backscatter material also taken from the slab phantom (s. fig. 2 and 3). Lateral positioning of the source relative to the chamber was facilitated by the concentric rings of the chamber holder. Fine positioning was realised afterwards by maximising the dose rate.

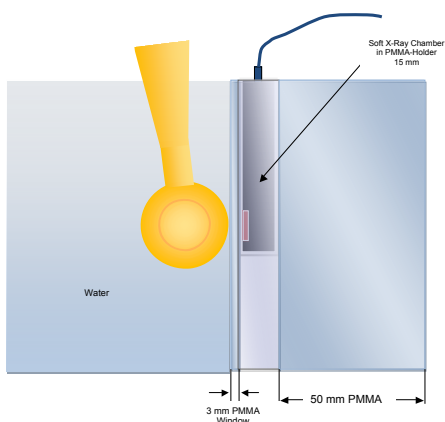
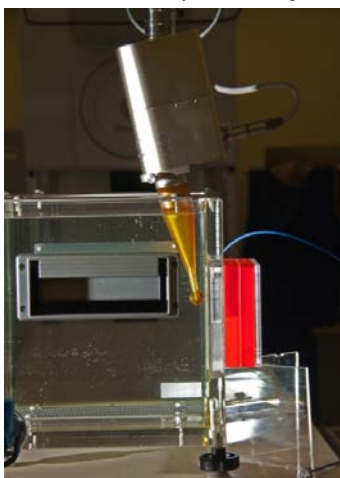


Fig. 3: Positioning of the source relative to the chamber.

Measurement of dose depth curves were performed with the same phantom and chamber set up, just moving the phantom moving relative to source driven by the table of our simulator.

Planar dose distributions around the different applicators were measured using Gafchromic EBT films in the water of the water tank as the accurateness and stability of these films have been proven by Avanzo et al. [9]. For this purpose the films were cut in the shape of the applicators so that these fit perfectly into the film (Figure 4a) and 4b)). For the evaluation an Epson Expression 10000 XL flatbed scanner and VeriSoft 4.0 were utilised.

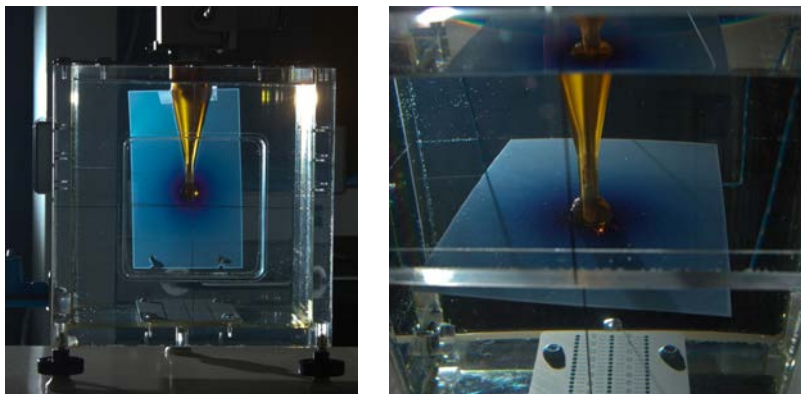


Figure 4a) and 4b): Measurement of polar (left) and azimuthal dose distributions around the intrabeam applicators with Gafchromic films in a water filled phantom.

In order to evaluate the environmental dose exposure we compared different survey monitors for consistency in reading, the stated energy ranges being 45 keV - 3 MeV for Automess AD 6150, 30 keV - 1.3 MeV for Berthold LB 123 H*(10) and 17 keV - 3 MeV for RadEye B 20 ER). The measurements were performed with a cylindrical phantom of 11 cm diameter, an applicator of 3.5 cm diameter thus having 3.75 cm of water to the surface of phantom at a height over ground equal to the height of the source. This way we tried to mimic the situation for an average breast treatment in lateral directions. Ambient dose was measured with and without additional shielding of the phantom to detect the effect of leakages and compared our findings with the declaration in the radiation protection brochure of Zeiss [10] for similar emission geometry. For this purpose we had to interpolate the data of Zeiss given at 1 and 2 m above ground to 1.5 m where our data were taken. The shielding drapes we used were those newly sold by Zeiss which have a specified attenuation equivalent to 0.25 mm Pb at 80 kV peak.

Inaccuracies of survey monitors could be revealed as being due to sensitivity effects at low energies that have to be expected as Intrabeam at 50 kV peak tube voltage produces a weekly filtered X-ray spectrum with a half value layer thickness (HVL) of 0.64 mm Al which is in between T30 (HVL = 0.42 mm Al) and T50 (HVL = 0.93 mm Al). The effective energy is ~20.4 keV. [11].

Results

Table 2 shows the results of the measurements of absolute dose. They are in accordance with the predictions of the treatment planning system and well within the tolerance interval we aimed at when configuring the method. Deviations result from inaccuracies in the mechanical positioning of the source relative to the chamber, which is extremely critical in soft X-ray dosimetry.

Applicator diameter / cm	TPS Dose / Gy	Measured Dose / Gy	Relative deviation
1.5*	5.13	5.27	2.7 %
2*	5.6	5.7	1.7 %
2.5*	6.19	6.42	3.7 %
3*	6.52	6.58	0.9 %
3.5**	6.0	5.77	- 3.8 %
4**	6.39	6.20	- 3.6 %
4.5**	6.7	6.53	- 2.5 %
5**	6.98	6.95	- 0.4 %

Table 2: Absolute dose measurements of Intrabeam in comparison with values predicted by the treatment planning system. One asterisk marks applicators marked with aluminium hardening filter whereas applicators without filter are marked with two asterisks. The discontinuity in the output of applicators above 3 cm is due to the change in filtering.

Our measurements of dose depth curves are shown in figure 5 as an example for the 2 and 4 cm applicators. The same finding was observed for the other applicators. Again we see a good agreement with the predictions of the manufacturer's basic data in the planning system.

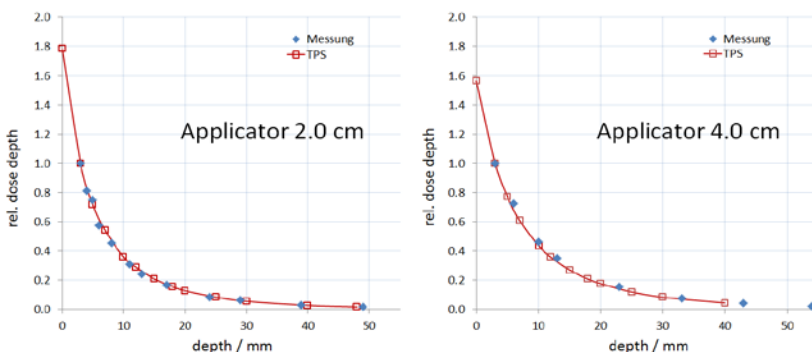


Fig. 5: Measured dose depth curves of two different applicators in comparison with the prediction of the Intrabeam treatment planning system

Isodoses of polar and azimuthal dose distributions are displayed in Figure 6. The observed centricity and spherical shape is well within clinical tolerance and gives rise to the assumption of a well-adjusted source.

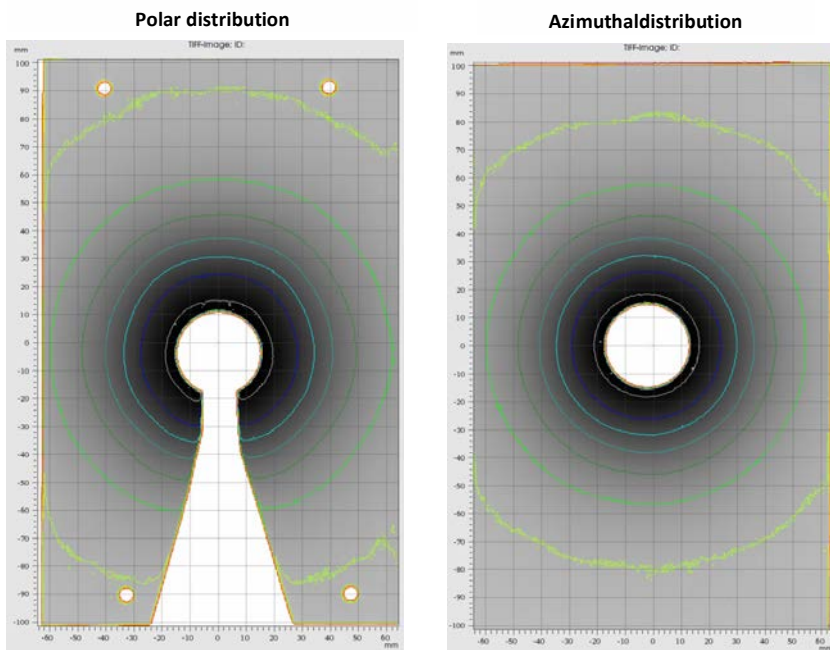


Fig. 6: Polar and azimuthal dose distributions as evaluated with VeriSoft®.

Discussion

Absolute dosimetry could be easily performed using the thin window of the PTW-4322 water tank with satisfying accuracy, if care was taken that the ion chamber was embedded in sufficient back scatter material. Even for a rough verification of soft X-ray dose depth curves no dedicated phantom was needed. The results show a good concordance with the pre commissioning data in the treatment planning system of IntraBeam® measured with a high precision phantom.

With Shielding (0.25mm Pb)				
Measuring Device	ZEISS (TLD)	RadEye B 20 ER	Berthold LB 123 H*(10)	Automess AD 6150
Min. Energy		17 keV	30 keV	45 keV
Distance/m				
1	1.3 mSv/h	2.0 mSv/h	380 µSv/h	140 µSv/h
1.5		800 µSv/h	190 µSv/h	61 µSv/h
2	400 µSv/h	400 µSv/h	110 µSv/h	35 µSv/h
3		150 µSv/h	49 µSv/h	18 µSv/h

Without Shielding				
Measuring Device	ZEISS (TLD)	RadEye B 20 ER	Berthold LB 123 H*(10)	Automess AD 6150
Min. Energy		17 keV	30 keV	45 keV
Distance/m				
1		28 mSv/h	5.0 mSv/h	1.9 mSv/h
1.5		11 mSv/h	2.3 mSv/h	900 µSv/h
2		5.7 mSv/h	1.4 mSv/h	420 µSv/h
3		2.3 mSv/h	630 µSv/h	170 µSv/h

Table 3: Ambient dose measurements with different survey monitors with and without the actually distributed shielding drapes in comparison with the declaration of Zeiss [10] captured with TLD for a shielding type no longer supported by Zeiss. Uncertainties of our data are estimated to be $\pm 10\text{-}20\%$ as common in radiation protection.

Film-dosimetry in a water tank using Gafchromic EBT films could be successfully used to verify the isotropy of the emission in the polar as well as the azimuthal plane thanks to the water stability of these films. This method was to our opinion quick, simple and comprehensive taking into account that commissioning has to be repeated in a very short time due to clinical demands whenever the source is being exchanged (in case of technical problems occurring more or less likely) or recalibrated (once a year). The former findings of G. Kunz et al. [8] are widely confirmed – the new generation of Intrabeam® sources seeming to perform a little better than the one this group worked with.

The clinical rollout indicated that elementary radiation protection issues are being underestimated relying completely on the documentation of the producer of Intrabeam® [10]. Data are given with a breast shielding that is no longer available and the predecessor can cause leakages. In an unshielded situation dose rates of nearly 2.5 mSv/h could be found at a realistic distance of 3 m meaning an ambient dose of > 1 mSv per average treatment. Consequently a room shielding of > 0.3 mm Pb (approximately 1.5 tenth layers) in total seems to be recommendable for a standard operation theatre of 6 x 6 meters square, if it is intended to offer the treatment frequently. Numerical calculations of radiation protection are somewhat unpleasant as attenuated direct radiation has to be considered, which is not covered by the Swiss X-ray ordinance and in contrast to common practice in Switzerland the vendor does not offer assistance in this field except the cited potentially misleading brochure. So the appropriate room shielding has to be determined experimentally when the device is already delivered. In our situation this lead to the decision of the executive radiation protection officer (J.B.) that the vitrification in the operating rooms, which were prepared for C-arm X-ray examinations in both hospitals, had to be reinforced by 0.5 mm of lead glass. Afterwards nowhere outside the operating rooms exposure rates of more than 30 µSv/h could be detected assuring a treatment of more than 100 patients per year without exposing the personal above the tolerable level. Radiation protection properties of the vitrification were of particular importance in our case because we decided that no personnel should be inside the room during treatment and thus in case of good performance the supervision of anaesthesia as well as the physical control of the radiation source could be easily done from outside.

Clinical experience of more than 40 patients shows that in total Zeiss Intrabeam® is a quite reliable and stable instrument for IORT with the advantage of a well assisted quality assurance procedure and integrated dose rate monitor. The handling of the source with the well balanced stand is very much appreciated by the operators and gives rise to a high degree of accuracy in positioning.

References

- [1] Vaidya JS, Joseph DJ, Tobias JS et al. *Targeted intraoperative radiotherapy versus whole breast radiotherapy for breast cancer (TARGIT-A trial): An international prospective randomised non-inferiority phase 3 trial.*, Lancet 2010; **376**: 91-102
- [2] Keshtgar MRS, Vaidya JS, Joseph DJ et al. *Targeted intraoperative radiotherapy for breast cancer in patients in whom external beam radiation is not possible.* Int J Radiat Oncol Biol Phys 2011; **80**:31-38
- [3] Vaidya JS, Baum M, Tobias JS et al. *Long-term results of targeted intraoperative radiotherapy (targit) boost during breast conserving surgery.* Int J Radiat Oncol Biol Phys 2011; **81**:1091-1097
- [4] Wenz F, Welzel G, Blank E et al. *Intraoperative radiotherapy as a boost during breast conserving surgery using low-kilovoltage X-rays: the first 5 years years of experience with a novel approach.* Int J Radiat Oncol Biol Phys 2010; **77**:1309-1314
- [5] Kraus-Tiefenbacher U, Bauer L, Scheda A et al, *Long-term toxicity of an intraoperative radiotherapy boost using low energy X-rays during breast conserving surgery* Int J Radiat Oncol Biol Phys 2006; **66**:377-381
- [6] Carl Zeiss Surgical GmbH, *INTRABEAM Präzision, die den Tumor trifft* (patient brochure) DE_30_010_151II
- [7] Carl Zeiss Surgical GmbH *INTRABEAM Produktspezifikation*, Brochure DE_30_101_1581 (2010)
- [8] Kunz G, Krayenhühl F, Streller T and Reiner B *Commissioning of a soft X-ray source for intraoperative breast cancer irradiation* Proceedings of the Annual Scientific Meeting of SSRMP 2008, Chur, ISBN 3 908 125 43 X
- [9] Avanzo M, Rink A, Dassie A et al. *In vivo dosimetry with radiochromic films in low voltage intraoperative radiotherapy of the breast.* Med Phys 2012 **39**:2359-2369
- [10] Carl Zeiss Surgical GmbH *INTRABEAM Informationen zur Strahlensicherheit*, Brochure DE_30_010_163I (2011)
- [11] Carl Zeiss Surgical GmbH *INTRABEAM Dosimetry*, Brochure EN_30_010_155II (2011)

O08

Surface dose optimization of the Varian Ir-192 HDR surface applicator set with vertical Leipzig-style cone

Konrad Buchauer, Hans Schiefer, Ludwig Plasswilm

Departement of Radiation Oncology, Kantonsspital St. Gallen, 9007 St.Gallen / Swizerland

Purpose: For clinical use of the Varian Ir-192 HDR surface applicator set with vertical Leipzig-style cone the manufacturer-provided table of treatment times for a given dose at 5mm depth is verified and extended to surface doses. Goal of our work is to evaluate the optimal source position to obtain a maximum therapeutical area and a depth dose characteristic suitable for clinical use. Additionally it is determined whether certain well known shortcomings from comparable brachytherapy surface applicator sets apply to the Varian surface applicator set as well and how the influence of dose inhomogeneity can be limited in clinical use.

Methods: The manufacturer provided time-dose table is verified with a calibrated PTW 0.3cc semiflexible ionisation chamber for two representative applicator inserts (20mm and 40mm diameter). For the extension of the 5mm reference depth dose in this table to surface dose a 0.02cc PTW soft X-ray chamber is used. High resolution 2D dosimetry is performed with Gafchromic film. Calibration of the films is performed in the reference geometry of the manufacturer with Ir-192 HDR irradiation with the 40mm diameter surface applicator. Dose is normalised in a region of interest similar to the projection of the 0.3cc ionisation chamber in the plane of measurement. For film scanning an Epson V700pro flat bed scanner in transparency mode is used.

Results: The manufacturer provided treatment time to dose table is well in agreement with our measurements, with a deviation smaller than 1%. Therapeutic area is defined as the area of the 90% isodose and found to be maximal with source position 10mm from the applicator tip for the applicator inserts 10mm to 25mm diameter, with a source position of 15mm from tip for all larger applicator inserts of the applicator set. A maximal therapeutic area on the surface is clinically given priority over a reduced depth dose resulting from using the 10mm position. In addition to known flatness problems of vertical type brachytherapy surface applicators a cold spot of size of approximately 3mm × 3mm with 70% of the nominal dose is found asymmetrically nearby the central axis of all applicators. Asymmetry of the dose distribution presumably arises from a slightly tilted source in treatment position. When alternation of the direction of the afterloader cable is performed from fraction to fraction to force the cable to a different angle in treatment position and when a position deviation of the central axis of ±1mm per fraction is assumed, the central axis region dose is actually 90%, what we consider as clinically acceptable.

Conclusions: Therapeutic area can be optimized with diameter dependent source positions. To limit the influence of the cold spot in the target area in clinical use systematic alternation of the direction of the cable is performed from fraction to fraction. Design of flattening filters similar as has been done for comparable applicator sets has to be considered in future use to improve the dose distribution homogeneity.

O09

Validation and evaluation of a collapsed cone dose calculation algorithm for HDR brachytherapy

Dario Terribilini(1), Werner Volken(1), Michael K. Fix(1), Kristina Lössl(2), Peter Manser(1)
(1) *Division of Medical Radiation Physics and Department of Radiation Oncology, Inselspital, Bern University Hospital, and University of Bern, Switzerland*
(2) *Department of Radiation Oncology, Bern University Hospital and University of Bern*

Introduction

Commonly, for dose calculations of HDR treatment plans the TG43 formalism is used. Since this formalism assumes an infinite water phantom as a basis for dose calculations, its accuracy is limited in certain conditions such as near the body contours or in presence of inhomogeneities. Nowadays, Monte Carlo (MC) methods are used to calculate dose distributions very accurately. However, due to their relatively long calculation time, MC methods are mainly used as benchmark for other dose calculation algorithms. An alternative is the collapsed cone (CC) dose calculation algorithm of Nucletron. In this work we present (1) a validation of the CC with MC and (2) an evaluation of the CC dose calculation on clinical breast cancer cases.

Method

In a first step, the brachytherapy source microSelectron mHDR v2 of Nucletron has been implemented in our MC environment (MC-Brachy) and a validation against published TG43 data has been performed. For this purpose, the dose in a spherical 80 cm diameter water phantom has been scored in a polar voxel geometry, which accounts for the symmetry of the source and partially compensates the loss of statistics given by the $1/r^2$ behavior of the dose distribution of a point source. Furthermore the CC algorithm has been validated by comparing the dose distribution in the same water sphere with the MC dose simulation as well as with TG43 data. For this validation the total doses as well as the single dose components calculated with CC and MC according to the primary and scatter dose separation (PSS) formalism have been compared. The second part of this work consists of the evaluation of the CC-algorithm using clinical cases. To accomplish this, clinical treatment plans for breast cancer patients have been selected and dose distributions have been calculated with CC and MC. For this evaluation identical input, i.e. media composition and physical densities assigned to the voxel phantom as well as all plan informations, for both algorithms have been used.

Results

At distances greater than 2 mm from the center of the source, MC agrees within 1% with the TG43 data and, thus, can be considered as a benchmark for the CC algorithm and any further brachytherapy dose calculation algorithm. The comparison between the CC algorithm and MC in the spherical water phantom shows that CC underestimates the deposited dose at distances between 2 and 8 cm from the source by at maximum 2% of the reference dose (dose in 1 cm from the source on its equatorial plane). At distances larger than 15 cm, CC overestimates the dose deposition; however, this difference is of no practical relevance. Calculated doses on clinical breast cancer cases performed with CC agree in general very well with dose distribution simulated with MC.

Conclusions

The CC algorithm is a very accurate dose calculation algorithm. Its implementation into brachytherapy improves dose calculation accuracy, particularly for situations where the TG43 formalism has some limitations.

O10

In-vivo thermoluminescent dosimetry assessment of target dose delivery using IMRT and VMAT in patients with ano-rectal cancer

*Dipasquale G, Nouet P, Rouzaud M, Dubouloz A, Sedmak C, Miralbell R, Zilli T
Radiation Oncology Geneva University Hospital, Geneva, Switzerland*

Objective

To assess the dose delivered to the target volume during IMRT or VMAT in patients with anal or rectal cancer using TLDs whose anatomical position was evaluated using CBCTs.

Material and methods

A new procedure was used to perform in-vivo dosimetry using TLDs placed in cavities in high- and low dose regions. Using CBCT images and image registration, TLDs were located respect to planned treatments, and expected dose estimated. We present the results of 8 patients treated with IMRT (n=1), VMAT (n=6) or both techniques (n=1) for ano-rectal cancer. Eclipse ver.10 was used for planning and patients were treated on a 2100C/D Varian linac equipped with on-board imaging. Five TLDs were fitted in a Rando phantom to evaluate TLDs readings contribution resulting from CBCT imaging.

Results

TLDs reading in the Rando phantom, after irradiation with a standard pelvis CBCT protocol, resulted in 2 cGy for all 5 TLDs, approximately 1% of the prescribed dose. These readings were neglected in the present analysis.

A total of 51 measurements (43 in the anal canal/rectum and 8 at the anal margin) were analyzed. Median planned and measured doses were 1.78 Gy (range, 0.15-2.01 Gy) and 1.80 Gy (range, 0.14-2.14 Gy), respectively. Overall, TLD doses measurements differed by a median dose of 0.01 Gy, ranging between -0.16 and +0.21 Gy (median difference in percentage of 0.5%, range - 8.9%/+11.7%) in comparison to the planned doses. Differences $\leq 5\%$ or $\geq 5\%$ between calculated and estimated doses were observed in 8 (15.6%) and 7 (13.7%) measures, respectively, but only 1 measurement was over 10%.

Conclusion

With high dose gradients in IMRT and VMAT treatments it is essential to know the correct position of TLDs in order to properly analyze the results of in vivo dosimetry. This new procedure seems dealing with this issue, allowing validating and monitoring doses delivered to patients.

O11

Definition of Parameters for Quality Assurance of Flattening Filter Free (FFF) Photon Beams in Radiation Therapy

*Antonella Fogliata, Alessandro Clivio, Giorgia Nicolini, Eugenio Vanetti, Luca Cozzi
Oncology Institute of Southern Switzerland, Bellinzona, Switzerland*

Purpose: Flattening filter free (FFF) beams generated by medical linear accelerators have recently started to be used in radiotherapy clinical practice. Such beams present fundamental differences with respect to the standard filter flattened (FF) beams, making the generally used dosimetric parameters and definitions not always viable. The present study will propose possible definitions and suggestions for some dosimetric parameters for use in quality assurance of FFF beams generated by medical linacs in radiotherapy.

Methods: The main characteristics of the photon beams have been analyzed using specific data generated by a Varian TrueBeam linac having both FFF and FF beams of 6 and 10 MV energy. Parameters related to profiles, depth dose curves, as well as linac output were studied for FFF beams together with the corresponding FF beams.

Results: Definitions for dose profile parameters are suggested starting from the renormalization of the FFF with respect to the corresponding FF beam. From this point the flatness concept has been translated into one of 'un-flatness' and other definitions have been proposed, maintaining a strict parallelism between FFF and FF parameter concepts.

Conclusion: Ideas for quality controls (QC) used in establishing a quality assurance program (QA) when introducing FFF beams into the clinical environment are given here, keeping them similar to those used for standard FF beams. By following the suggestions in this report we foresee that the introduction of FFF beams into a clinical radiotherapy environment will be as safe and well controlled as standard beam modalities using the existing guidelines.

O12

Weekly QA of linac dosimetry using a 2-D detector array

*Natacha Ruiz Lopez, J.-F. Germond, R. Moeckli
Institute of Radiation Physics, Lausanne University Hospital, Lausanne*

We have successfully implemented a protocol for performing all the weekly dosimetry part of the linac QA required by the SSRMP recommendation N°11 for photons and electrons using PTW 2D-array or StarcheckMaxi supplemented by a homemade wedged beam quality (BQ) phantom.

The system [1] allows to measure in one shot per modality and energy the absolute central axis dosis (tests 3.1 and 4.1 of recommendation N°11), the transverse and longitudinal asymmetry, the homogeneity (tests 3.11 et 4.8) and the energy (tests 3.10 and 4.7). This device fulfills the requirement of recommendation N°11 because a) the calibration of the device is metrologically traceable to METAS, b) it is made of water equivalent material and c) all the dosimetry tests are included.

The beam energy is evaluated by analyzing diagonal profiles measured under a copper wedge for photons and two opposing aluminium wedges for electrons. In order to demonstrate that this type of analysis gives values of energy free from instrumental bias, we have analytically modeled the relation between profiles under a wedge and depth dose curve for electrons. The calculated full width half maximum of the profiles EC_{FWHM} under the aluminium wedges is related to the half-value depth in water R_{50} by the linear relation:

$$EC_{FWHM} / 2 = a + b \cdot R_{50}$$

where, to first order approximation, the coefficients a and b are given by

$$b = 1 / (\rho_{Al}^{rel} \cdot tg\alpha) \quad \text{with } \alpha = \text{angle of the aluminium wedge}$$

$$a = x_0 - z_d \cdot b \quad \text{with } x_0 = \text{wedge offset and } z_d = \text{depth of measurement}$$

Predictions of these formula for energies between 4 and 15MeV agree within 3% with our simultaneous best fit to data taken with the Siemens Primus and Elekta Synergy CHUV linacs which gives $a=3.30\pm0.02$ cm and $b=0.781\pm0.006$. We have also shown that a better agreement is obtained when using the complete model based on the analytical parameterization of electron depth dose curve proposed by Strydom [2] and of the mass stopping power ratio of the SSRPM recommendation N°10.

In summary, ionization chamber arrays coupled to a wedged phantom provides an efficient and well modeled device for weekly dosimetry QA. All the procedure for 2 photons and 5 electrons energies can be performed by entering the irradiation room only twice and in about 20 minutes. The procedure is also easily adaptable to other 2D detectors such as EPID.

Further work will be done for determining relationship between our measurements and $TPR_{20,10}$ parameter for energy check.

[1] R.J. Speight, A. Esmail, S. J. Weston, J Appl Clin Med Phy 12 (2012) 239

[2] WJ Strydom, Med Phys 18 (1991) 1254

O13

Results from testing the Octavius pre-treatment QA system equipped with the inclinometer

*Eugenio Vanetti, Alessandro Clivio, Antonella Fogliata, Giorgia Nicolini, Luca Cozzi
Oncology Institute of Southern Switzerland, Bellinzona, Switzerland*

Purpose: The Octavius (PTW) pre-treatment QA system is now equipped with an inclinometer device, able to provide information on the gantry position during an arc treatment delivery. In the present study the capabilities of this system for RapidArc (RA) pre-treatment QA have been investigated.

Materials and Methods: Five RA plans made up of one complete arc have been selected, presenting different modulation levels. Pre-treatment QA measurements were done with the 729 ionization chambers detector array (PTW) inserted into the Octavius phantom. A 6MV beam from a UNIQUE (Varian) linac equipped with MLC-120 Millennium was used. Each measurement was repeated with the octagonal phantom placed in its 8 possible positions (one per each supporting side). In this way the detector and the Octavius hollow laid in all possible positions. For each image acquired with the inclinometer, the contribution from a definable gantry angular interval is determined by the associated PTW Verisoft software. Pre-treatment QA was evaluated in the present study for the original full arc and for given gantry angular intervals, distinguishing the sectors irradiating the detector array laterally, the phantom from its anterior position and through the Octavius hollow. Acquired contribution was compared with the corresponding calculated dose image. Calculations were done in the Varian Eclipse planning system using Acuros XB algorithm. Comparisons between acquired and calculated dose images have been performed through the gamma analysis (DTA=2mm and $\Delta D=1\%$, 2% and 3% on a global basis) using the Verisoft software, in the defined sectors.

Results: Gamma analysis results of complete arcs cases were always satisfactory at least for the conditions with $\Delta D=2\%$ and 3%: the percentage of points fulfilling the gamma criteria, called gamma agreement index (GAI), was 97%. Results concerning gantry intervals highlighted differences: very good agreement was shown for sectors orthogonal to and in front of the detector, where the GAI was greater than 90% also for $\Delta D=1\%$; for sectors irradiating the detector laterally the GAI was lower than 95% only for $\Delta D=1$ and 2%.

Conclusion: The use of the inclinometer together with the Octavius system allowed investigating the behaviour of the 729 detector respect to different sectors of RA arcs. In general the system behaves adequately for the most irradiation conditions investigated. Only for small sectors the results becomes suboptimal. With the different positions of the Octavius phantom and the inclinometer, an accurate pre-treatment QA is possible for all sectors.

O14

Dosimetric properties of an amorphous silicon EPID for verification of modulated electron radiotherapy

Cécile Chatelain(1), Daniel Vetterli(1), Daniel Morf(2), Dominik Henzen(1), Pascal Favre(1), Michael K. Fix(1), Peter Manser(1)

(1) Division of Medical Radiation Physics and Department of Radiation Oncology, Inselspital, Bern University Hospital, and University of Bern, Switzerland

(2) Varian Medical Systems Imaging, Laboratory GmbH, Baden-Dättwil, Switzerland

Purpose: To investigate the dosimetric properties of an electronic portal imaging device (EPID) for electron beam detection and to evaluate its potential for pre-treatment quality assurance (QA) of modulated electron radiotherapy (MERT).

Methods: A commercially available EPID was used to detect electron beams shaped by a photon multileaf collimator (MLC) at a source-surface distance of 70 cm. The fundamental dosimetric properties such as reproducibility, dose linearity, field size response, energy response and saturation were investigated for electron beams. A new method to acquire the flood-field for the EPID calibration was tested. For validation purpose, open fields and various MLC fields (square and irregular) were measured with a diode in water and compared to the EPID measurements. Finally, in order to use the EPID for pre-treatment QA of MERT, a method was developed to reconstruct EPID 2D dose distributions in a water-equivalent depth of 1.5 cm. Comparisons were performed with film measurement for static and dynamic mono-energy fields as well as for multi-energy fields composed by several segments of different electron energies.

Results: The advantageous EPID dosimetric properties already known for photons as reproducibility, linearity with dose and dose rate were found to be identical for electron detection. The flood-field calibration method was proven to be effective and the EPID was shown to accurately reproduce the dose measured in water at 1.0 cm depth for 6 MeV, 1.3 cm for 9 MeV and 1.5 cm for 12, 15 and 18 MeV. The deviations between output factors measured with EPID and in water at these depths were within 1.2%. The average gamma pass rate (criteria: 1.25%, 1.25 mm) for profile comparison between EPID and water measurements was better than 97% for all the energies considered in this study. When comparing the reconstructed EPID 2D dose distributions at 1.5 cm depth to film measurements, the gamma pass rate (criteria: 2%, 2 mm) was better than 97% for all the tested cases.

Conclusion: This study demonstrates the high potential of the EPID for electron dosimetry, and in particular, confirms the possibility to use it as an efficient verification tool for MERT delivery.

This work has been accepted for publication in Medical Physics (2013).

O15

Physical Aspects of Total Skin Electron Irradiation at the University Hospital Basel

Götz Kohler, Roman Menz, Renate Nyffenegger, Frank Zimmermann

Klinik für Strahlentherapie und Radioonkologie, Universitätsspital Basel, Basel, Switzerland

Total skin electron irradiation (TSEI) was done last time in Basel in 1995. This year we implemented again TSEI in our department. The procedure was different from the previous one for several reasons. Therefore, the setup was a new implementation.

The TSEI treatment was performed on an Elekta precise linac. The patient was treated in an upright position with a focus skin distance of 4 m at the reference point. In contrast to previous TSEI treatments in our institution no electron applicator was used to get the fields as wide as possible and to get the highest dose rate available. A dual field technique was applied with a 72° and a 108° gantry beam direction.

A 6 mm thick PMMA plate covering the whole patient was used to reduce electron energy as well as to work as a scatter foil. The nominal electron energy was 6 MeV at the highest possible dose rate of 700 MU/min, corresponding to 0.35 Gy/min at the reference point.

Due to the large distance and the PMMA plate a reduction of the electron energy to about 4 MeV can be assumed. Percent depth dose was determined with a Roos chamber in a solid water slab phantom. Beam profiles were also measured in a slab phantom at a depth of 1 cm as well as on the surface. Profiles varied over a length of 1.6 m (patient's height) between 97.6% and 101.9%.

To get a homogeneous skin dose the patient was positioned in six different orientations (each as dual field) with an angle increment of 60°, three of them treated each day resulting in a two days period for the complete plan. A wooden frame was built in house in order to get an appropriate positioning and stability of the patient standing upright within the frame. The patient was treated with a fraction dose of 1 Gy per day on average. Before the treatment radiochromic measurements were performed in an *Alderson phantom* in three planes: in the mid plane, in the shoulder area as well as in the head area in order to check the homogeneity of the dose distribution around the patient.

In vivo measurements were done using diodes as well as radiochromic films in order to check the skin dose. Finger and foot nails were protected with a 2 mm lead shield. No eye lens shielding was applied as the patient had already artificial lenses.

Some skin areas which were underdosed were additionally treated daily with orthovoltage therapy using 100 kV and 150 kV depending on the location on the patient.

O16

Interplay effect between respiratory motion and dynamic irradiation: Experimental test of a simple analytical model

J.-F. Germond, S. Thengumpallil, R. Moeckli

Institute of Radiation Physics, Lausanne University Hospital

In order to achieve the best possible conformality of treatments, modern radiotherapy make ample use of dynamic delivery techniques such as sliding windows, dynamic wedges and dynamic arc therapy. These techniques have been experimentally commissioned by dose measurements in static phantoms and are routinely validated for patient treatments in the same way. However this ideal dosimetry picture is tarnished in the thorax region by the internal motion of the patient organs due to respiratory and cardiac automatisms. For static fields delivered in a time lapse larger than the respiratory cycle, this results in the blurring of dose distribution and possible geometric misses due to baseline shifts of the tumor. For fields involving dynamic collimation, the delivered dose distribution will in addition be locally increased or decreased depending on the synchronisation between the leaves movements and the respiratory cycle. This is referred as the interplay effect [1].

The present study aims at experimentally testing a previously published [2] analytical model in the special case of dynamic wedges. Dose delivered by an Elekta Synergy™ linac were measured with a PTW 2D-array seven29™ sited on an in-house dynamic platform allowing 1D periodic movement up to 3 cm in amplitude with variable frequency. A wedge dynamic 2 control points DICOM RT-Plan linearly closing the leaves of a 20x20 field was generated and used for dose measurements for a set of different MU's values. One of the major limitation of dynamic delivery by leaves measurements being their speed limit, the internal beam delivery system has to adjust the dose rate (in our case by definite steps) in order to respect this limit. This in turn modifies the impact of the interplay effect and leads to an apparent complex pattern.

Our measurements confirm that this complex pattern varies in space with a periodicity equal to the product of the leaves speed by the cycle length in full agreement with the analytical model. The measured maximum variation of the interplay factor (ratio of dose with and without motion) at normal respiratory rate reaches 25% for leaves moving at 1.5 cm/s and 8% at half this speed and scales linearly with the cycle length. Detailed confrontation of our measurements with the model is showing some discrepancies related to the non ideal behaviour of the irradiator (penumbra in profiles) and the presence of medium scatter.

In summary, we have confronted our measurements to a previously published [2] analytical model of the interplay effect and found an overall agreement. This type of analysis, if generalized to rotational techniques such as VMAT or Tomotherapy™, could be useful for regular QA of dynamic delivery. The analytical model predicts also that the new faster MLC proposed by vendors could force us to incorporate the interplay effect in the planning process itself.

[1] T. Bortfeld et al., Phys. Med. Biol. 47 (2002) 2203.

[2] C.X. Yu, D.A. Jaffray and J.W. Wong, Phys. Med. Biol. 43 (1998) 91.

O17

Investigation of the dose accuracy and benefits of gated IMRT and VMAT for clinical implementation

*Angèle Dubouloz, Coline Corbet, Dolores Leduc
University Hospitals of Geneva, Geneva, Switzerland*

Purpose: To evaluate the dose accuracy and benefits of gated intensity modulated radiation therapy (IMRT) and gated volumetric modulated arc therapy (VMAT) for clinical implementation.

Methods and materials: The Dynamic Thorax Phantom from CIRS (DTP) was used for this study. The phantom mimics a human thorax and contains a moving and programmable rod enclosing a spherical tumor in the left lung. Thirteen different settings were tested combining three spheres of different diameters (1, 2 or 3 cm) and seven breathing patterns. One 4D-CT (BigBore, Philips) per setting was acquired using the Real-time Positioning Management system (RPM, Varian). Due to the regularity of the respiratory movement, a phase-based reconstruction was used rather than an amplitude-based reconstruction. The breathing cycle was split into 10 phases and the phases where the tumor had the least movement were chosen for the study. Gated and non-gated 7-field IMRT and 1-arc VMAT treatment plans were calculated with Eclipse 10.0. The prescription dose was 60 Gy at the target mean, in 30 fractions. Absolute dose measurements were performed with thermoluminescent dosimeters (TLD, diameter 2 mm, thickness 0.1 mm) and 2D relative dose distributions were measured with radiochromic films (Gafchromic EBT3, ISP). Fifty-two dose-volume histograms (DVH) were analyzed and compared.

Results: The differences between absolute calculated and measured doses were smaller than 3%. The 2D dose distribution was assessed using a gamma criterion of 3%/3mm. The passing rate of 95 % was achieved in the majority of gated and non-gated IMRT and VMAT plans. The comparison showed that the reduction in dose to organs at risk was important for high amplitude pulmonary movements (> 5 cm). For amplitudes of 5 cm, 10.2 % of healthy lung tissue receiving 20 Gy was spared with IMRT and 9.7 % with VMAT compared to non-gated treatments. The size of the tumor appeared to be an important selection criterion: the volume of healthy tissue spared increased with tumors volume. An IMRT plan of a 1 cm diameter tumor with 1 cm amplitude preserved less than 2 cm³ of healthy tissue. The same treatment plan for a 3 cm diameter tumor with 5 cm amplitude spared at least 55 cm³ of healthy tissues.

Conclusion: The commissioning of this new technique was satisfying. IMRT and VMAT gating should only be used clinically for large and mobile tumors to obtain the greatest dosimetric benefit and to counterbalance the decrease in patient comfort due to the longer treatment delivery time. For all other cases, deep inspiration breath hold treatments using RPM appeared to be the best solution but could not be studied with the DTP.

O18

First tests with a new 6 degrees of freedom couch

Daniel Schmidhalter(1), Michael K. Fix(1), Marcel Wys(2), Niklaus Schaer(2), Peter Munro(2), Stefan Scheib(2), Martin Amstutz(2), Peter Manser(1)

(1) Division of Medical Radiation Physics and Department of Radiation Oncology, Inselspital, Bern University Hospital, and University of Bern, Switzerland

(2) Varian Medical Systems Imaging Laboratory GmbH, Baden, Switzerland

Introduction – In radiotherapy, accurate patient setup is of great importance and has an impact on normal tissue sparing and/or permit dose escalation. In recent years, image-guided radiotherapy has been successfully implemented in clinical routine. Typically, a 4 degrees of freedom (4DoF) couch is used to apply the shifts assessed by imaging systems. However, the use of a 6 degrees of freedom (6DoF) couch has the potential to further improve patient setup accuracy. In this work, we tested a pre-released version of a new 6DoF couch from Varian Medical Systems.

Materials/Methods – The new 6DoF couch is based on the existing TrueBeam™ couch with an additional 2DoF module for pitch and roll rotations. The 2DoF module is 12 cm high, can handle a maximum load of 200 kg, does not reduce the vertical travel range of the existing couch, can pitch and roll $\pm 3.0^\circ$, has no mechanical assemblies extending into the rotation volume of the gantry head, uses no external devices (e.g., optical cameras) to control its position and is integrated completely within the TrueBeam™ control system. The tests performed in this study were based on the comparison between intended shifts and the measured shifts after the intended shifts have been applied, using a variety of methods (imaging system, digital inclinometer and room laser system). For each of the six axes, the performance of the 6DoF couch was separately tested. Fabricated and clinically relevant situations were investigated using a cube phantom and an anthropomorphic head phantom, respectively. Both phantoms were placed at positions typically used during clinical applications as well as at extreme positions, where possible setup inaccuracies due to the couch are assumed to be maximized. Shifts in the range of ± 3 cm (translational axes) and $\pm 3^\circ$ (rotational axes) were applied. All tests were performed for different couch loads up to 200 kg.

Results – Over all measurements, the deviations (mean \pm one standard deviation) between the intended and the measured shifts verified by the imaging system, digital inclinometer and room laser method were -0.01 ± 0.02 cm, 0.00 ± 0.02 cm and 0.00 ± 0.02 cm for the longitudinal, lateral and vertical axis, respectively. The corresponding values for the three rotational axes couch rotation, pitch and roll were $0.01 \pm 0.05^\circ$, $-0.02 \pm 0.08^\circ$ and $-0.01 \pm 0.06^\circ$, respectively. The deviations presented here result from different error sources where the inaccuracy of the 6DoF couch itself is only one of them. No significant difference between the tests without and with a couch load of up to 200 kg was observed.

Conclusion – The study shows that the new 6DoF couch is able to apply intended shifts with high accuracy. It has the potential to be used for treatment techniques requiring the highest demands in patient setup accuracy such as those needed in stereotactic treatments.

O19

Implementation of a Monte Carlo model for dose calculations in small animal imaging at TOMCAT beamline

Silvia Peter(1,2), Goran Lovric(1,2), Michael K Fix(3), Werner Volken(3), Daniel Frei(3), Peter Manser(3), Marco Stampanoni(1,2)

(1) Paul Scherrer Institut, Villigen, Switzerland

(2) Institut for Biomedical Engineering, ETH Zürich, Zürich, Switzerland

(3) Division of Medical Radiation Physics and Department of Radiation Oncology, Inselspital, Bern University Hospital and University of Bern, Bern, Switzerland

In-vivo tomographic imaging is an important contemporary topic of research at the beamline for Tomographic Microscopy and Coherent radiology experiments (TOMCAT) [1]. One example is functional 3 dimensional lung imaging. So far in-vivo lung imaging has only been achieved in 2D or with low spatial and temporal resolution, therefore in-vivo, high-resolution tomographic imaging remains an open topic [2]. An important aspect for such in-vivo measurements is the radiation dose delivered to the animal which, depending on the goal of a study, can be a limiting factor. Thus, an accurate knowledge of the dose accumulated by the animal is necessary prior to any imaging study. However, given the high flux at imaging beamlines of third generation synchrotron facilities, dosimetry is a challenging task. A convenient way to estimate the dose to the animal is to perform Monte Carlo (MC) simulations.

In this work a MC model of the TOMCAT beamline has been implemented for the purpose of dose estimation in in-vivo small animal tomography. All beam defining elements in the beam path were included in the model which was implemented using *egs++*[3]. To obtain an estimation of the dose distribution within an animal, two phantoms were implemented: a water phantom which consists of a water cylinder and a small animal phantom, which consists of a soft tissue cylinder with inserts of air and bone to represent the lungs, the ribs and the spine of the small animal. For both phantoms, calculations for different set-ups that may occur in an experiment were performed and analyzed. Three energy settings were considered: a 21 keV mono-energetic beam, a 5% filtered white-beam and a 0.5% filtered white-beam. The results show that the maximal relative dose was accumulated in the region of interest for the water phantom and in the bones for the small animal phantom. This model can now be used to improve the experimental set-up for in-vivo tomography with respect to the accumulated dose.

References

- [1] M. Stampanoni et al. Trends in synchrotron-based tomographic imaging: the SLS experience, Proc. of SPIE (2006) Vol. 6318
- [2] A. Fouras et al. The past, present, and future of x-ray technology for in vivo imaging of function and form, J. Appl. Phys 105, 102009 (2009)
- [3] I. Kawrakow et al. The EGSnrc C++ class library, NRC Report PIRS-898 (rev A), Ottawa, Canada (2009)

O20

Assessment of the exposure of the Swiss population to computed tomography

Abbas Aroua(1), François O Bochud(1), Reto Meuli(2), Barbara Ott(3), Elina Samara(1), Reto Treier(3), Philipp R Trueb(3), Francis R Verdun(1)

(1) Institute of radiation physics, Lausanne University Hospital, Rue du Grand-Pré 1, CH-1007, Lausanne, Switzerland

(2) Department of Diagnostic and Interventional Radiology, Lausanne University Hospital, Rue du Bugnon 21, CH-1011 Lausanne, Switzerland

(3) Radiation Protection Division, Federal Office of Public Health, CH-3003, Bern, Switzerland

Background and Objective: The frequency of computed tomography (CT) procedures has registered a significant increase over the last decade; CT is now contributing significantly to the total collective dose due to medical X-rays: around 50% for developed countries. This work aimed at investigating the use of computed tomography in Switzerland. The frequency and dose data related to CT and their trend are assessed, analyzed and compared to the figures reported in the literature.

Methods: The whole community of CT users in Switzerland was addressed within the framework of a nationwide survey on the exposure of the population by radiodiagnostics. A total of 238 CT units are concerned. The hospital departments and radiology institutes were asked to fill a questionnaire either online or on paper form, and provide the annual number of procedures they performed in 2008. The data collected from the respondents was projected to the national level by using the ratio of the number of participating units to the total number of units. The relative change of the number of CT examinations during the period 2008-2011 is assessed using a sample of representative hospitals. The average doses per CT procedure were established during an auditing campaign.

Results and discussion: In 2008 about 0.8 Million CT procedures (100/caput) were performed in the country, leading to a collective effective dose of more than 6000 man.Sv (0.8 mSv/caput). In a decade the frequency of CT examinations averaged over the population and the associated average effective dose per caput increased by a factor of 2.2 and 2.9 respectively. Although the contribution of CT to the total medical X-rays is 6% in terms of the frequency, it represents 68% in terms of the collective effective dose. These figures are comparable to those reported in a number of countries in Europe and America with similar health level. The frequencies of CT examinations continue to increase from 2008 to 2011.

O21

Clinical Audits in RADIOLOGIE in Switzerland

Carine Galli Marxer, Reto Treier, Philipp R. Trueb

Division Radioprotection, Federal office of Public Health, Bern, Switzerland

The mission of the Federal office of Public Health (FOPH), and more precisely of its radioprotection division, is to protect the Swiss population. A special sensitive group are patients being exposed to ionizing radiations from medical treatment techniques, as well as the medical staff operating these installations.

In light of this fact, the FOPH performs different activities. For instance the quality assurance and the radiation shielding of radiological facilities are examined during technical audits. In the past diagnostic reference levels (DRL) have been published so that doses applied to patients can be optimized by the different radiological centers. Nevertheless, despite all these efforts, the exposure of the Swiss population by medical X-rays in the diagnostic radiology increased of 20% in 10 years, reaching 1.2 mSv per inhabitant in 2008.

The computer tomography (CT) plays a central role in this dose increase since it is responsible for more than 2/3 of the collective dose, although it represents only 6% of the frequency of all radiological exams. Several studies show that up to 30% of the CT performed on young patients aren't justified [Eur Radiol 2009, 1161]. Moreover, even in the case of a justified CT, non-justified phases are performed for more than half of the patients [JACR 2011, 756]. In Switzerland, several actions have shown that it is possible to decrease the delivered doses by adjusting the CT protocols depending on the patient size [Spital Oberengadin, 2012] as well as by teaching the personal [Radiologie 2010, 1120].

Other studies have also shown that radiologists as well as non-radiologists have the tendency to underestimate the delivered doses and associated risks of ionizing radiation [Rad Prot Dos 2011, 1; R6Fo 2007, 261].

Therefore, the FOPH started officially in 2011 a project to introduce clinical audits in RADIOLOGY, that comprises the diagnostic radiology, the nuclear medicine and the radio-oncology. The aim of the project is to insure the optimal use of ionizing radiation for patients. In concrete terms, it means that exams have to be justified, that all radiological processes and associated resources have to be optimized, and that the clinical personal as well as patients have to be aware of the radioprotection thematic.

Such clinical audits have already been introduced in 1997 in the European legislation [97/43Euratom], and are based on a peer-review system, where physicians, medical physicists and radiographers will evaluate the practice of another radiological center. Finland already audited all its radiological centers twice, and their experience is very positive.

In Switzerland, the Swiss ordinance on radioprotection is currently revised, and a new article concerning the clinical audits will be included. During the last year, a working group containing the main stakeholders analyzed the Swiss situation, and defined as well the content of the new legislation. These results will be presented during the meeting.

O22

Image quality characterisation of time-of-flight and point-spread-function corrections in the PET/CT Discovery-690

*S. Gnesin(1), J. Delacoste(1), P. Martinez(1), M. Pappon(2), J.O. Prior(2), F. Verdun(1),
(1) Institute of radiation physics, Lausanne University Hospital, Lausanne, Switzerland
(2) Department of nuclear medicine, Lausanne University Hospital, Lausanne, Switzerland*

Introduction and motivations:

Recently, several innovations become available for commercial PET devices potentially increasing the quality and the quantitative accuracy of PET images, in particular: the 3D acquisition mode, the time of flight (TOF) information and the point spread function (PSF) corrections.

TOF-based reconstruction algorithms allow in principle a more precise localization of the annihilation site along the concerned line of response leading to noise reduction and improvements in image contrast and spatial resolution.

Spatial resolution in PET suffers from intrinsic (positron range + non-collinearity of annihilation photons) and detector-related degradation factors (finite energy resolution + depth of interaction).

Phantom-based and clinical studies showed that the inclusion of the PSF correction in the iterative image reconstruction process leads to appreciable recovery of the spatial resolution by reducing partial volume effects; additionally noise reduction and increased contrast are also observed.

Material and methods:

In this work we characterised the performances of TOF and PSF corrections in terms of Recovery Coefficients (RCs), image noise and contrast. The study was performed on a GE Discovery 690 PET/CT (GE Healthcare) where ^{18}F -FDG filled standard NEMA IEC phantoms were imaged using clinical reconstruction setting. We also explored the possible quantitative bias induced by the use of the PSF correction.

Results:

TOF (as compared to non-TOF reconstructions) increases the cold sphere contrast (+15%) while it does not affect significantly the contrast of hot lesions. No appreciable benefit of the TOF is found in terms of background noise reduction estimated by the coefficient of variation (COV). PSF correction (as compared to non-PSF corrected images) improves RCs and contrast in particular for small (<10 mL) hot sphere, a significant COV reduction (-20%) is also reported. Quantitative bias (potentially affecting SUV quantification) is observed at the edge of large (>10mL) cold lesions, and the PSF correction typically overestimate the measured activity concentration at the hot spheres periphery as compared to the center and leads to RC overestimation ($\text{RC}_{\text{max}} > 1$) with an average activity overestimation of 6%.

Conclusions:

Our phantom study shows the impact of TOF and PSF corrections on PET image quality according to lesion contrast and size which is the basis for further clinical characterisation.

O23

Involvement of medical physicists in diagnostic radiology and nuclear medicine

Treier Reto, Zeller Werner, Trueb Phillip R.

Federal Office of Public Health, Radiation Protection Division, Bern, Switzerland

In Switzerland, the working field of medical physicists in clinical routine has so far been limited to radio-oncology only. This was due to legal requirements since only in radio-oncology there has been a legal obligation for license holders to employ medical physicists for quality assurance, supervision of accelerator operation and therapy planning (Art. 19¹, Linear Accelerator Ordinance). With the introduction of Art. 74⁷ of the Radiological Protection Ordinance (RPO), which came into force on January 1 in 2008 and for which a 4-years transitional period has been granted for implementation, medical physicists must periodically be enlisted in diagnostic radiology (computed tomography and fluoroscopy-guided interventional radiology) and for nuclear medicine applications. This paper provides an overview of the practical implementation of Art. 74⁷ from the viewpoint of the Federal Office of Public Health (FOPH).

The objective of Art. 74⁷ is to optimize the radiation protection of patients and staff for high-dose procedures in diagnostic radiology and nuclear medicine. In order to achieve this aim areas of optimization and tasks of medical physicists must be specified in detail. A joint working group consisting of representatives of the involved professional societies (SSR, SSNM, SSIPM, SVMTRA, SSRMP, SGRRC), the industry and the FOPH developed guidelines and recommendations for the application of 74⁷ which were published in a report in June 2011 (<http://www.bag.admin.ch/themen/strahlung/02883/02885/index.html?lang=de>). This report has been recognized by all stakeholders as basis for the uniform implementation in Switzerland. Three principle areas of optimization have been defined: (1) quality assurance relating to patient dose (measurements of appropriate patient/occupational/public safety related dosimetric quantities; a repetition of quality tests already performed by manufacturers is explicitly excluded), (2) verification and optimization of patient and staff doses (improving patient protection by optimization of practices, procedures and acquisition protocols; improving protection of medical staff by giving advice on machine operation and use of protective equipment) and (3) training and coaching of technologists and physicians (theoretical training courses and/or practical on-site coaching).

Actually, each of the 265 license holders affected by Art 74⁷ submitted a concept of implementation to the FOPH. Different kinds of concepts have been presented: in-house concepts (medical physicists of a radio-oncology department provide the service within the hospital only); networks/cantonal concepts (medical physicists of a (newly created or already existing) radiation protection unit provide the service within a canton or network of radiology departments or institutes); private service providers. The actual status of implementation is very inhomogeneous, some service providers already started their first visits and data collection whereas others haven't yet started at all. The FOPH is in close contact to all service providers to provide support during the practical implementation if required. At the end of this year or beginning of next year, the FOPH plans to organize a joint symposium with the service providers to exchange first experiences and discuss possible problems encountered. Such a symposium may also provide valuable input for the revision of the RPO whose implementation is scheduled for autumn 2014.

O24

Diagnostic Reference Levels in Nuclear Medicine – an Update for Switzerland

Hans W. Roser

University of Basel Hospital, Radiological Physics, Basel, Switzerland

Introduction

Diagnostic Reference Levels (DRL) serve as a reference to the user of ionizing radiation in diagnostic radiology and nuclear medicine. They should reflect the state-of-the-art possibilities of balancing the radiation dose to the patient and the necessary imaging quality. Accordingly the DRL have to be reassessed periodically, since equipment and experience progress and change quickly. A survey in Switzerland – carried out in 2004 – was the base to establish the nuclear medicine DRL in 2006 [1]. They have been in use since and a new survey in 2010 was conducted to help upgrade the existing DRL. The project was supported by the Federal Office of Public Health (FOPH).

Material and Method

In 2010 we carried out a survey in all nuclear medicine centers – 54 in total – in Switzerland to assess data on the application of radioactive nuclides to the patient. We acquired age, sex, weight, type of procedure, activity and if applicable complementary CT data for more than 8'500 patients. We extracted statistical information on the frequencies of the applications and the applied activities. Together with a support group of representatives of the involved professional disciplines and the FOPH we worked out an updated set of DRL.

Results

There have been marked shifts in the frequencies of the procedures since the last survey in 2004. Bone scans still are the most frequent procedures (28%), followed by PET (21%) and myocardial procedures (18%). In 2004 the corresponding numbers were 40%, 8% and 23% respectively. The new DRL haven't changed by much, however for some of the procedures it is planned to introduce – in addition to the "plain" DRL – values in relation to the weight of the patient.

Discussion

While the new DRL will soon be published in an update of the existing leaflet [1], the FOPH – on the basis of the recommendations of the support group – also wants to partly extend the information to the user by weight related values. In this context it is intended to strengthen our recommendations for the applications to children with reference to the proposal made on this matter by the European Association of Nuclear Medicine [2]. Likewise it is planned to make public the 25., 50. and 75. percentiles of the activity distributions according to the survey, so the user can better judge her/his location in the spread of applied quantities of radioactivity to the patient.

References

- [1] Bundesamt für Gesundheit: Diagnostische Referenzwerte (DRW) für nuklearmedizinische Untersuchungen, Weisung L-08-01 vom 30. Januar 2006
- [2] F. Jacobs, H. Thierens, A. Piepsz, K. Bacher, C. Van de Wiele, H. Ham, R.A. Dierckx. Optimised tracer-dependent dosage cards to obtain weight-independent effective doses. *Eur J Nucl Med Mol Imaging* (2005) 32:581–588.

M01

Evaluation of the 'worst case scenario' approach to handle setup uncertainties in proton treatments

Margherita Casiraghi(1,2), Francesca Albertini(1), Antony John Lomax(1,2)
(1) Center for Proton Therapy, Paul Scherrer Institut, 5232 Villigen PSI, CH
(2) Department of Physics, ETH Zürich, 8093 Zürich ETH-Hönggerberg, CH

Intensity-Modulated Proton Therapy is a powerful proton treatment delivery technique which provides a highly conformal dose distribution. However, due to the steep dose gradients produced, IMPT can be also very sensitive to the treatment delivery uncertainties. Therefore, it is important to include the robustness criterion in the plan evaluation process. Thanks to its simple implementation, one of the most used method to model dose errors is the 'worst case scenario', i.e. the worst realizations of the patient treatment uncertainties cause the largest dosimetric errors that can occur during the plan delivery.

We tested the worst case scenario hypothesis, in the case of setup errors, by validating the 'Dose Error-Bar' tool developed at PSI Center for Proton Therapy. The tool allows the visualization of a dose error-bar associated with every voxel of the nominal dose distribution. The magnitude of the error-bar corresponds to the difference between the maximum and the minimum of the dose values coming from the recalculation of the plan on a number of worst case patient positioning scenarios. For the validation, we uniformly sampled spatial shifts from a spherical space of radius equal to the worst case patient misalignment. A number of treatment scenarios were simulated and the dose deviations from the nominal dose distribution were computed and compared to the dose error-bar distribution.

The punctual comparison shows the dose error-bars are a correct estimation ($\pm 5\%$) of the potential dose errors for the 96% and 85% of the irradiated voxels, respectively for a skull-base and a spinal-axis IMPT. The voxels in which the model fails are localized near to soft tissue-bone interfaces and air cavities. Additionally, we compared the simulations and the dose error-bar distributions by the means of Error-Volume Histograms and Dose-Volume Histograms. We showed that the percentage of a given structure that is subjected to a certain maximum dose error can be correctly estimated from the EVHs obtained from the DEB tool and the DVHs of the worst and best dose distribution always represent the lower and upper bound of the plan quality when setup uncertainties within a certain confidence interval are considered.

To conclude, the assumption that the larger patient shifts lead to the worst dose distributions does not necessarily hold punctually. Nevertheless, for the tested cases, the voxels in which the model fails are a low percentage of the total irradiated volume and when performing a volumetric analysis, the quality of the plan can be correctly estimated by evaluating the plan just for a limited number of worst case scenarios. Thus, we believe that the DEB tool and the more general worst case scenario model can be introduced in the IMPT planning procedure. Given that photon plans are less sensitive to medium heterogeneity, the use of this model can be extended, with less limitations, to the evaluation of intensity-modulated photon treatment robustness.

M02

Monitor units are not predictive of neutron dose for high-energy IMRT

Roger A. Halg(1), Jurgen Besserer(1), Markus Boschung(2), Sabine Mayer(2),
Uwe Schneider(1,3)

(1) Institute for Radiotherapy, Radiotherapie Hirslanden AG, Aarau, Switzerland

(2) Division for Radiation Safety and Security, Paul Scherrer Institut, Villigen, Switzerland

(3) Vetsuisse Faculty, University of Zurich, Zurich, Switzerland

Due to the substantial increase in beam-on time of intensity-modulated radiotherapy techniques to deliver the same target dose compared to conventional treatment techniques, an increased dose of stray radiation is delivered to the patient. In the case of high energy photon radiotherapy (>10 MV nominal energy), secondary neutrons are produced in the gantry head, which are an additional contribution to the stray dose of a patient. It is commonly assumed that the neutron dose equivalent scales with the beam-on time and therefore with the number of applied monitor units. As a consequence, an increase in second malignancies may be expected in the future with the application of intensity-modulated radiotherapy.

Measurements of neutron dose equivalent were performed using PADC track etch detectors in a solid water phantom for an open and an intensity-modulated field. The open irradiation field was defined by the collimator jaws with the MLC retracted, whereas the intensity modulation was done by a sweeping MLC gap with the jaws in the same position as for the open field. The same absorbed photon dose was applied for the two fields with a monitor unit ratio of three. The neutron dose equivalent was determined at four positions: inside and outside of the treatment field at 0.2 cm and 15 cm depth, respectively.

It was shown that the neutron dose equivalent, which a patient receives during an intensity-modulated radiotherapy treatment, does not scale with the ratio of applied monitor units relative to an open field irradiation. Outside the treatment volume at larger depth, 35% less neutron dose equivalent is delivered than expected.

In conclusion, this study showed that the predicted increase of second cancer induction rates for the neutron stray dose from intensity-modulated treatment techniques can be overestimated when the neutron dose is simply scaled with the number of monitor units applied.

M03

Measurements of whole-body dose distributions in radiotherapy for different treatment machines and delivery techniques

Roger A. Halg(1), Jurgen Besserer(1), Uwe Schneider(1,2)

(1) Institute for Radiotherapy, Radiotherapie Hirslanden AG, Aarau, Switzerland

(2) Vetsuisse Faculty, University of Zurich, Zurich, Switzerland

Contemporary radiotherapy treatment techniques such as intensity-modulated radiation therapy and volumetric modulated arc therapy increase the beam-on time needed to deliver the same dose to the target and irradiate a larger volume with low doses compared to conventional treatment techniques. This could lead to an increase of radiation-induced malignancies for these new techniques. In this study, whole-body dose distributions from typical radiotherapy patient plans using different treatment techniques and therapy machines were measured. The same measurement-setup and irradiation intention were applied to allow a direct comparison of the measured stray doses.

Individually calibrated thermoluminescent dosimeters were used to measure absorbed dose in an anthropomorphic phantom. The dose distributions from photon beams with a nominal energy of 6 MV were compared in terms of treatment technique (3D-conformal, intensity-modulated radiation therapy, volumetric modulated arc therapy, helical TomoTherapy, stereotactic radiotherapy, hard wedges and flattening filter-free radiotherapy) and therapy machine (Elekta, Siemens and Varian linear accelerators, Accuray CyberKnife and TomoTherapy).

Close to the target, the doses from treatments using intensity modulation (including flattening filter-free) were below the dose from a static treatment plan, whereas the CyberKnife showed a larger dose by a factor of two. Far away from the treatment field, the dose from intensity-modulated radiotherapy treatments showed an increase in dose from stray radiation of about 50% compared to the 3D-conformal treatment. For the flattening filter-free photon beams, the dose from stray radiation far away from the target was slightly lower than the dose from a static treatment. The CyberKnife irradiation and the treatment using hard wedges increased the dose from stray radiation by nearly a factor of three compared to the 3D-conformal treatment.

This study showed that the dose outside of the treated volume is influenced by several sources. Therefore when comparing different treatment techniques, the dose ratios vary with distance to the isocenter. The effective dose outside the treated volume of treatments using intensity modulation with or without flattening filter was 10 to 30% larger when compared to 3D-conformal radiotherapy. This dose increase is much lower than the monitor unit scaled effective dose from a static treatment.

M04

Direct aperture optimization concept for inverse planning of modulated electron radiotherapy

*Dominik Henzen(1), Peter Manser(1), Daniel Frei(1), Werner Volken(1),
Hans Neuenschwander(2), Ernst J. Born(1), Michael K. Fix(1)*

*(1) Division of Medical Radiation Physics and Department of Radiation Oncology, Inselspital,
Bern University Hospital, and University of Bern, Switzerland*

(2) Clinic for Radiation-Oncology, Lindenhofspital Bern, Switzerland

Introduction: Due to the steep dose fall off of electron beams at larger depths, electron radiotherapy is suitable for tumour sites near the surface with distal organs at risk (OARs) to be spared. The possibility of multi leaf collimator (MLC) shaped fields and modulated electron radiotherapy (MERT) would surpass the current application techniques for electrons routinely used by means of efficiency and conformity. Subsequent to the development of an electron beam model for MERT treatment planning [1] and a forward planning strategy [2], the development of an inverse planning strategy is a consequential proceeding. However, this is work in progress and herewith we would like to present the concept, current status and preliminary results.

Concept: For the inverse planning process, a direct aperture optimization (DAO) approach [3] employing a simulated annealing algorithm has been implemented. For each iteration in the DAO random changes have been tested to the initial apertures. The dose distribution given these new apertures has then been calculated. A cost function (CF), summing up the squared differences between the actual dose values in a structure and a user specified dose limit, has been evaluated in order to decide whether or not the update will be accepted. For a decreasing CF value the new apertures have been accepted and the next iterations starts. If the CF value increased, there is a probability to accept the new apertures and dose distribution, otherwise the changes of the apertures and hence the dose distribution remains unchanged, i.e. the modification has been rejected. This probability has been given by the simulating annealing algorithm. To update the dose distributions efficiently, a set of ‘beamlets’ has been defined and the dose deposition for each beamlet has been pre-calculated and stored in a file. Therefore, after each aperture change, the dose from the beamlets, which have been opened or closed, will be subtracted from or added to the prior dose distribution. First tests using an academic situation containing a planning target volume (PTV) and a distal OAR have been carried out.

Discussion: The current implementation is able to successfully generate a treatment plan for the academic situation. Further investigations and improvements will be undertaken in order to obtain a robust and flexible inverse planning algorithm for complex clinical cases.

Conflict of Interest: This work was supported by Varian Medical Systems.

References: [1] Henzen D, Manser P, Frei D, Volken W, Neuenschwander H, Born E J and Fix M K : “Efficient Monte Carlo based Electron Beam Model for MERT using a Photon MLC”, ICTR-PHE 2012, Geneva

[2] Henzen D, Manser P, Frei D, Volken W, Neuenschwander H, Born E J and Fix M K : “Forward planned MERT using the Swiss Monte Carlo Plan”, SASRO 2012, Winterthur

M05

Eye-Tracking human observers in lung CT volumetric detection tasks

*Ivan Diaz(1), Sabine Kobbe-Schmidt(2), Francis R. Verdun(1) and François O. Bochud(1)
(1) Institute of Radiation Physics, Lausanne University Hospital, Lausanne, Switzerland
(2) Department of Radiology, Lausanne University Hospital, Lausanne, Switzerland*

Anthropomorphic model observers are mathematical algorithms which seek to mimic the detection performance of humans in order to quantify image quality and to run large scale optimization trials that wouldn't be practical otherwise. The development of model observers has progressed from very simple detection tasks to tasks involving detection of realistic signals in complex two-dimensional backgrounds. Many medical imaging modalities are now three-dimensional, and model observers need to take volumetric aspects into account. In clear, this means that the temporal effects of image scrolling are particularly important. In CT, radiologists search across slices in a volume and their eyes fixate on different locations while scrolling the slices at different speeds. In this work, we looked at lung nodules because they are very difficult to distinguish from blood vessels unless the slices before and after the current one are used for comparison. Thus, the temporal aspect is particularly important and has been used to get an idea of the way radiologists and naïve observers incorporate the use of different slices when detecting signals.

We performed a series of 3D 2-AFC (Alternative Forced-Choice) detection tasks on volumetric stacks of CT lung images. That is, two side-by-side sets of images were shown with exactly one of the two containing the signal, and the observers were asked to identify with the computer mouse which one it was. The signal was extracted from a positive lung case and embedded in manually extracted healthy lung backgrounds. Each set was 21 slices deep with the image size 128x128 and when the signal was present it was located in the middle. All the images were reviewed by a radiologist to ensure that they were realistic. The strategy used by radiologists and naïve observers was assessed using an eye-tracker. In a first set of experiments, the observers were restricted to read the images at three fixed speeds of image scrolling and were only shown each alternative once. They were then allowed to scroll through the image stacks at will. We were able to determine a histogram of scrolling speeds in frames per second. From this, the average speed, speed just prior to detection and speed around the signal could be determined. From observing radiologists looking through real cases, they tend to quickly scroll back and forth around the signal before making a decision. The scrolling speed at the moment the signal was detected was estimated at 20 fps. This was higher than that reported by the radiologists.

M06

Combining wave-optics and Monte Carlo methods for the simulation of grating based hard X-ray interferometry

Silvia Peter(1, 2), Peter Modregger(1, 3), Michael K Fix(4), Werner Volken(4), Peter Manser(4), Marco Stampanoni(1, 2)

(1) Paul Scherrer Institut, Villigen, Switzerland

(2) Institute of Biomedical Engineering, ETH Zürich, Zürich, Switzerland

(3) School of Medicine and Biology, University of Lausanne, Lausanne, Switzerland

(4) Division of Medical Radiation Physics and Department of Radiation Oncology, Inselspital, Bern University Hospital and University of Bern, Bern, Switzerland

Hard X-ray grating interferometry (GI) is a recently established phase-sensitive imaging technique, which has the advantage of simultaneously providing three complementary types of contrast: absorption, phase and dark-field contrast [1,2]. Phase-contrast has been shown to offer a high sensitivity towards electron density variations and is, therefore, well suited for imaging soft tissue matter in the field of biomedical research [3]. However, there are still open questions about the image formation process, for example details of the dark-field contrast formation process are yet unknown.

For a realistic simulation of the image formation process both particle-like and wave-like properties of X-rays have to be considered, since phase contrast relies on beam coherence and dark-field contrast relies on scattering. On the one hand, wave-optics simulations are a well suited method for simulating coherent effects such as phase-shift and interference, but scattering cannot be modeled in a straight forward way. Monte Carlo methods (MC), on the other hand, are a convenient way to model scattering and absorption, but wave-like properties such as interference are generally not taken into account.

We have developed and validated a simulation framework that combines MC with wave-optics, thus taking into account both particle- and wave-like properties. The first step of the simulation, which models the source and the sample, was implemented using MC. In a second step propagation between the gratings was simulated by using wave-optics. To take into account the phase-shift of X-rays passing through the sample, the refraction process and the optical path length were included in the MC part. The phase-space of particles which result from the MC part, is transformed into a complex amplitude through a transition routine, which treats the particles as plane waves that are coherently summed up. In the wave-optics part the amplitude is propagated through the gratings and the complementary contrasts are obtained using a Fourier-based approach [1].

To validate the framework comparisons between simulations and measurements of a phantom were performed. The validation shows excellent agreement between simulation and experiment ($R^2 > 0.93$) and establishes the developed numerical framework as a reliable technique to model GI. Since refraction as well as scattering such as Compton and Rayleigh scattering are included in the framework, it can be used for detailed investigations of the scattering within a sample and, hence, to gain a deeper understanding of the dark-field image formation process.

References

- [1] T. Weitkamp et al, X-ray phase imaging with a grating interferometer, *Opt. Express* (2005) 13, 6296
- [2] A. Momose et al, Demonstration of X-Ray Talbot interferometry, *Jpn J Appl Phys.* (2003) 42:L866–L868
- [3] S. McDonald et al, Advanced phase-contrast imaging using a grating interferometer, *J. Synch. Rad.* (2009) 16, 562

M07

Respiratory-correlated cone beam CT as a pre-treatment tool for free breathing lung treatment: a phantom study

S.Thengumpallil(1), J-F. Germond(1), J. Bourhis(2), F.Bochud(1), R. Moeckli(1)

(1) Institute of Radiation Physics, Lausanne University Hospital, Lausanne

(2) Radio-oncology department, Lausanne university Hospital, Lausanne

Linac gantry-mounted CBCT used for image guided radiotherapy requires acquisition time of minutes, leading in the thorax region to blurred tumor images and possible erroneous baseline shifts in patient positioning [1]. Respiratory-correlated CBCT systems (4D-CBCT) overcome this limitation by retrospective sorting the images frames with respect to the diaphragm position, yielding 3D datasets, each corresponding to a certain breathing phase. One advantage of this 4D technique is that the breathing signal required for phase sorting, is directly extracted from the 2D projection data, thus removing the need for an external respiratory system. Linac 4D-CBCT allows to reduce respiration-induced geometrical uncertainties by monitoring, prior to treatment, the mean position, trajectory, and shape of a moving tumor.

The aim of this project is to implement workflow for free-breathing-lung treatments exploiting both 4D-CT (Aquillon LB Toshiba) and 4D-CBCT (Elekta Symmetry) acquisitions.

As first commissioning step, three types of phantoms were used: the CatPhan 503, the ANZAI for image quality assessment and the Octavius for dose measurements. The CatPhan 503 and the Octavius were imaged on a dynamic platform allowing 1D linear movement, while for the ANZAI the moving head simulates the $1D \sin^4$ movement. The image quality performance of CBCT and 4D-CBCT in static (3D) and dynamic (4D) modes were assessed with the CatPhan 503 for the low and medium reconstructions algorithms. The CBCT dose measurements were performed in the Octavius using an AISL ionisation chamber.

The ANZAI was also used to calculate the performance of image registration between the acquired 4D-CBCT images (10 phases) and the planning 4D-CT (Mid-position phase [2]). This system shall be considered as a QA tool for the overall patient workflow since it handles both the acquisition and the registration of 4D-CBCT images, prerequisite to a better control of the tumor intra- and inter-fraction baseline shift. For this purpose the acrylic sphere of the ANZAI was used as a moving tumor in a VMAT plan calculation (CMS Elekta Monaco TPS V. 3.1).

Our results showed a clear suppression of motion blurring artefacts when 4D-CBCT acquisitions are performed, but an increase of streak artefacts outside the tumor when a reduction in number of frame per phase is applied. We measured a kV dose ratio $\sim 7\%$ between the 3D-CBCT and the 4D-CBCT. The Symmetry system showed a good synchronization between 4D-CBCT and 4D-CT. It also provides a useful visual check of the target coverage as well as a safe verification of the selected planning phase (Mid-position).

The analysis presented here will be repeated and validated for patients, in order to guarantee and optimize PTV margins for the free-breathing lung treatments.

[1] Sonke et al. Med. Phys. **32** (2005)

[2] Wolthaus et al. Med. Phys. **35** (2008)

M08

Portal Dosimetry verification for VMAT: a comparative study of two methods

*Paolo Zucchetti, Regina Seiler
Luzerner Kantonsspital, Luzern, Switzerland*

Introduction

Epiqa™ and Varian’s Portal Dosimetry provide two methods for RapidArc™ plan verification by use of the portal imager (EPID). While Epiqa™ doesn’t require a particular imager calibration [1], it is affected by it, if one chooses to concurrently use Varian’s Portal Dosimetry, which does require a calibration [2]. Varian’s Portal Dosimetry solution was made available for RapidArc™ in 2011. It compares EPID images with calculated images. In our case, the calculated images are obtained using Eclipse™’s portal dose image prediction algorithm PDIP [3]. Initial tests in our institute did not show the expected results. Since this method works very well for IMRT, the aim of this work was to determine what the problem was for RapidArc™, and whether there are ways to achieve similarly good results as for IMRT. The ultimate goal of this work was that the patient specific plan verification could be performed with the portal imager instead of a 2D array in a phantom.

Material and Methods

Portal Dosimetry is absolutely calibrated with a fixed dose rate (600 MU/min) corresponding to the nominal dose rate of VMAT plans, although during the delivery of RapidArc™ plans this dose rate is rarely achieved. Since this is different to IMRT where actual dose rate and calibration dose rate are the same, it raised the question whether this discrepancy has an impact on the Portal Dosimetry evaluation.

To investigate this problem two plans were created in Eclipse. First a rotational plan with 11 rotational fields, which have an energy of 6MV and a field size of 10x10 square centimeters.

Field	1	2	3	4	5	6	7	8	9	10	11
Doserate [MU/min]	100	150	200	250	300	350	400	450	500	550	600
Number MU	125	187	250	312	375	437	500	562	625	687	750

Tab. 1: Parameters of the rotational fields

These fields are distinguished by the number of monitor units (MU), which were calculated using the following formula to obtain the desired various dose rates:

$$MU = \overline{DR} \cdot t \qquad t = \frac{359.8^\circ}{4.8^\circ/\text{sec}} \approx 74.96 \text{ sec} \approx 1.25 \text{ min}$$

The second plan consists of eleven static fields, which have an energy of 6MV, a field size of 10x10 square centimeters and a dose rate of 600MU/min for all fields. The only variable parameter is the number of monitor units.

Field	1	2	3	4	5	6	7	8	9	10	11
Doserate [MU/min]	600	600	600	600	600	600	600	600	600	600	600
Number MU	125	187	250	312	375	437	500	562	625	687	750

Tab. 2: Parameters of the static fields

These eleven fields are planned at gantry position zero and they have the same number of monitor units as the fields of the rotational plan. Based on these two plans two Portal Dosimetry verification plans were created. Those two plans were delivered at one of our Clinac iXs and a portal image was acquired for each of the 22 fields. The analyses of the acquired images are done using Varian's 'Portal Dosimetry' application. The CU values at the central axis of the acquired fluence images and the calculated image signals were analyzed.

The investigation of the data showed the need for a new absolute calibration of the PortalVision™ imager. For this reason, the measurements of the verification plans are repeated with the new absolute calibration and evaluated again.

After the investigation of the problem using the standard geometry with open fields without dynamic MLC, we verified the VMAT treatment plans of some patients. In this study, 75 patient-specific quality assurances were performed using Varian Portal Dosimetry (a total of 127 fields). For each verification plan two integrated images were acquired, one with the manufacturer's recommended calibration and the other with the new calibration.

Evaluation was performed using the gamma index method [4] with gamma criteria 3% dose difference and 3mm distance-to-agreement (DTA), which we currently use for our patient specific QA.

In addition, the DTA criterion was set to 1mm, and the dose-difference criterion was varied from 3% to 1%, in order to emphasize evaluation of the signal itself since geometric uncertainties shouldn't depend on the calibration method. In the analysis, signal values less than 10% of the maximum value were not evaluated.

Results

For the standard geometry, the analyses of the portal images were done using Varian's 'Portal Dosimetry' application. The mean signal in an area of two-by-two centimeter square around the central axis was compared to the corresponding calculated one.

For both plans and all fields the deviation between acquired and calculated imager signal was plotted as a function of the number of monitor units.

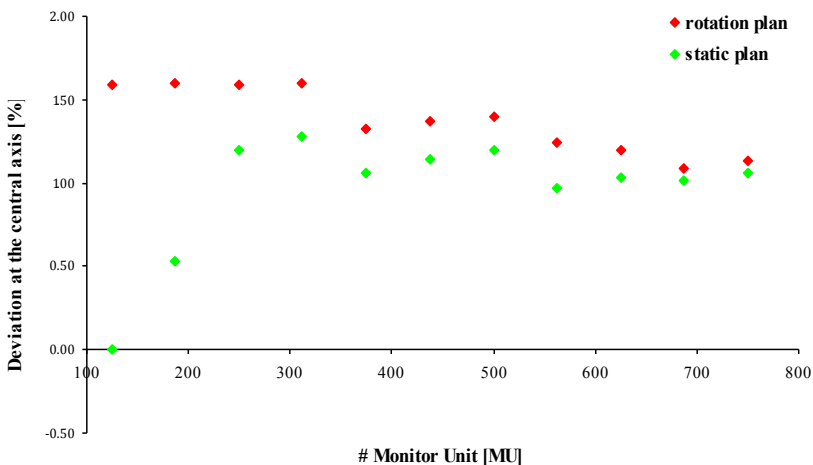


Fig. 1: Deviation between calculated and acquired fluence as a function of the monitor units for the rotation and static plan.

In the case of the static field we do have a good agreement between predicted and acquired image for 125 Monitor Units. This result was actually expected, as the portal imager was calibrated with a static field with 100 Monitor Units and a 600MU/min dose rate. However, a considerable deviation is observed for more monitor units and for the rotation plan in general. Above 250 monitor units this deviation remains almost constant.

These findings resulted in the idea to calibrate the portal imager in another way. The new calibration is carried out with the standard geometry, but instead of using 100MU we chose 400MU and set the corresponding signal to 4CU. There were two reasons for this: first, the average number of monitor units per field of all patient specific verification plans studied in this work is located in this region and secondly the deviation of 400MU represents the behavior observed above 250MU. After the new imager calibration, all fields were irradiated and evaluated again.

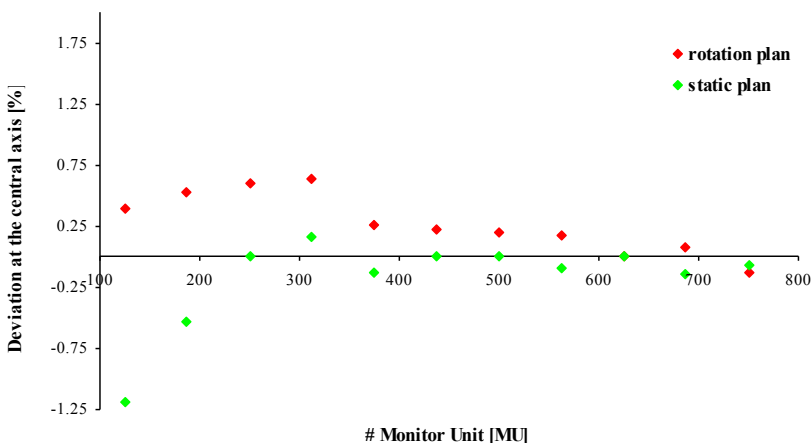


Fig. 2: Deviation between calculated and acquired fluence as a function of the monitor units for the rotation and static plan using the new calibration.

After the new calibration, the deviations for the static fields are close to 0% with the exception of low monitor units. The deviations for the rotation plan have become smaller. The increased deviation for static fields with low monitor units is not a concern for us since no static fields are verified with a dose rate of 600MU/min.

While the standard geometry with open fields without dynamic MLC showed good results, the real test lies in the actual VMAT plan QA. 75 VMAT plans were evaluated with the old and the new calibrations. Evaluation was performed using the gamma index method with gamma criteria 3% and 3 mm.

For each field, the percentage of pixels with a gamma index less than 1 is an indicator for the agreement between calculation and acquisition. The analysis is considered passed if 95% of all evaluated pixels have a gamma index of less than or equal to 1.

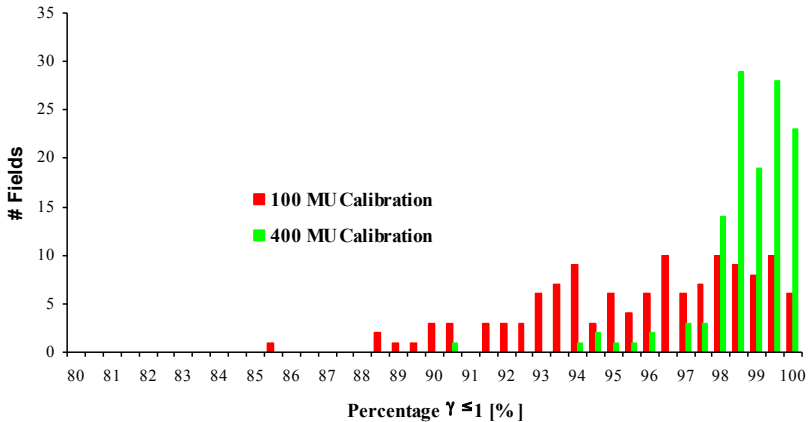


Fig. 3: Gamma criteria 3% and 3mm; both calibrations

With our clinical gamma criteria of 3mm and 3% an improvement in the overall agreement is clearly visible for the new calibration method.

With the standard calibration only 65% of all evaluated fields passed the analysis while with the new calibration almost 97% of all fields passed the analysis.

These results are very satisfying for our routine work, but in the course of this study more focus was set on the signal difference. It is assumed that any geometrical uncertainty is independent of the calibration method. Distance-to-agreement was therefore set to 1mm in order to avoid that a pixel was considered passing only because another pixel in its neighborhood had a similar signal.

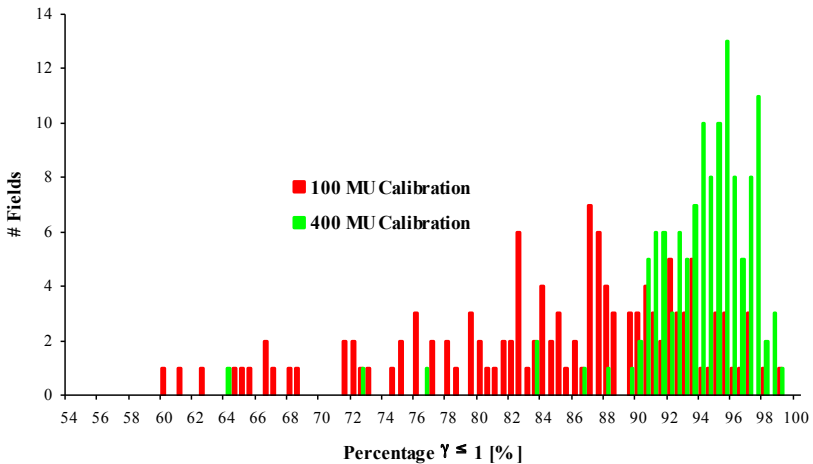


Fig. 4: Gamma criteria 3% and 1mm; both calibrations

With a tight distance-to-agreement the outcome is the same, confirming that the new calibration does improve the evaluation.

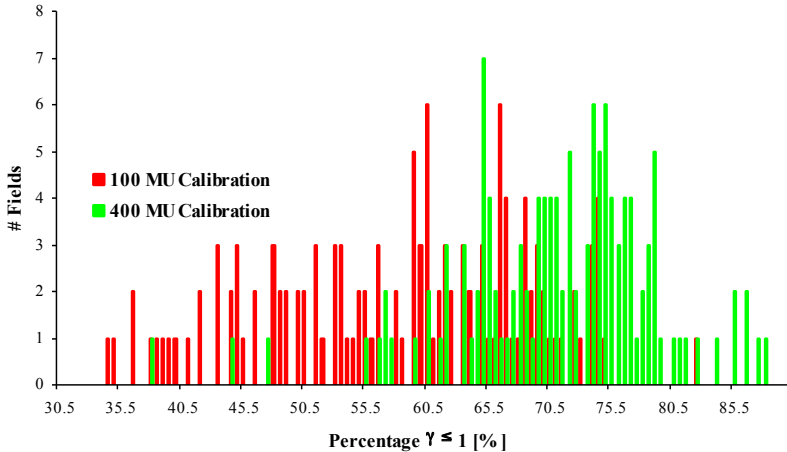


Fig. 5: Gamma criteria 1% and 1mm; both calibrations

As expected the overall agreement is decreasing when the gamma evaluation is pushed further by lowering the difference to 1%. Nevertheless, even with these criteria the new calibration gives better results.

Discussion

This work has shown that the new calibration improves Portal Dosimetry verifications. Not only are the results better, but they have actually become acceptable for routine use, making the time consuming setup with the 2D-array obsolete. For a few months now we have been verifying our VMAT plans with Portal Dosimetry and are satisfied with the outcome.

The findings of the investigation presented here have been communicated to Varian Medical Systems. Varian confirmed that these results are explained by the fact that the last partial frame of the integrated acquisition was not considered in the imaging acquisition system IAS3 [5]. Depending upon the total number of frames acquired, this effect has a larger or smaller impact. Typically, the error is more pronounced for the calibration at 600MU/min than for the calibration at 200-400MU/min. Increasing the number of monitor units for the CU calibration lessens the error as more frames are acquired, therefore reducing the offset of QA plans in general.

References

- [1] EPI dos, s. r. o. (2011). Epiqa, Reference Guide
- [2] Varian Medical Systems. (2007). Portal Imaging and Portal Dosimetry, Reference Guide - 8.1
- [3] Varian Medical Systems. (2011). Eclipse Algorithms, Reference Guide
- [4] Low, D. A., & Dempsey, J. F. (2003). Evaluation of the gamma dose distribution comparison method. [Comparative Study, Evaluation Studies, Research Support, Non-U.S. Gov't, Research Support, U.S. Gov't, P.H.S., Validation Studies]. *Med Phys*, 30(9), 2455-2464

P01

Dose Distribution Analysis of Small Fields in Electron Beam Therapy using Radiochromic Films

L. De Abreu Vieira(1,2), G. Kohler(2)

(1) Universitätsspital Basel, Radiation-Oncology Department, Switzerland

(2) Kantonspital Aarau, Radiation-Oncology Department, Switzerland

Even if there already exist excellent electron beam radiotherapy planning systems, it is still common to perform electron beam therapy planning by means of tables including percent depth dose (PDD) tables and the dose at the maximum, even so at the University Hospital of Basel (USB, Basel, Switzerland). However, Electron Beam Dose Distribution is not specified only by PDD. While planning via PDD is sufficient for field sizes larger than approx 4 cm (energy-dependency), off-axis ratios (OAR) might be significantly affected by small fields.

Additionally, individual applicator inserts are used which also can also affect dose distribution. Therefore, supplementary information about the electron dose distributions is also required for both small and large regular field sizes as well as for irregular inserts. The primary goal of the current work was to extend the present tables for electron beam treatment planning at the USB. The second goal was to implement a simple and fast method to perform fast dose distribution analysis. This work presents the development and standardization of a method to perform dosimetric analysis of electron beam dose distribution by means of radiochromic films at the USB.

P02

Case report: IMRT plan verification in homemade phantoms for Ewing sarcoma treatment around a distant femoral implant.

*Dipasquale Giovanna, Dubouloz Angèle, Nouet Philippe
Radiation Oncology Geneva University Hospital, Geneva, Switzerland*

Objective

A 33 year old patient with Ewing sarcoma who underwent surgery and distant femoral implant replacement was referred to our center for radiotherapy treatment in July 2012. The aim of the treatment was curative and consisted in irradiating the tissues in contact and surrounding the metallic implant to a dose of 50.4 Gy in 28 fractions. An IMRT dose shaped donut plan was created (7 fields, 6MV).

Using a cylindrical sample of the implant, two phantoms were used hosting it, to use for mini TLDs pretreatment dose verification.

Material and methods

The sample (MEGASYSTEM-C, LINK Implants AG, Bern) was first introduced in a cubic water equivalent phantom, adapting it using wax. An anterior and two lateral open fields plan was created to test the algorithm results (AAA, Eclipse version 10.0 Varian Medical System). Nine mini TLDs (2 mm Ø, 0.1 mm thickness) were positioned around the central axis before the sample, in contact, 2 TLDs at 4 mm from the surface and other 2 TLDs at 4 mm in the same direction but after the implant. A similar setup was used to test the IMRT plan, with gantry angles fixed to 0°. To take into account possible dose compensations in a symmetric irradiation, the CIRS electron density head phantom was used to simulate the leg containing the prosthesis (fitted in the central heterogeneity element with ≈ 1 mm wax), for IMRT plan verification with gantry rotation. For each cardinal position 3 TLDs were positioned in contact with the metallic sample in the central fields region.

Results

Cubic phantom: For the open fields plan, the contact surface median planned and measured doses were 1.78 Gy (range, 1.78-1.92 Gy) and 2.00Gy (range, 1.86-2.26 Gy), respectively. Doses differed by a mean of 10.8% (SD: 4.7%) in comparison to the planned doses. This discrepancy was reduced to -2.3 % (SD: 3.2%) before the metallic sample and to -0.3% (SD: 4.7%) after it, at 4 mm distance from its surface.

For the IMRT plan (all fields gantry angle set to zero), the largest dose difference was measured at the entrance contact surface, mean +23.9% (SD: 4.4), while for the exit contact it inverted sign, but reduced to -11.2% (SD: 0.7). This important difference was not present at 4 mm distance from the implant surface, -0.4 % (SD: 4.3%) before the metallic sample and -4.2% (SD: 0.7%) after it.

CIRS Phantom: For the IMRT plan verification using gantry rotation, 12 measurements were analyzed, with TLDs in contact with the metal implant. Median planned and measured doses were 1.66 Gy (range, 1.47-1.76 Gy) and 1.69 Gy (range, 1.42-1.83 Gy), respectively. Doses differed by a mean of 1.5% (SD: 2.9%) in comparison to the planned doses, showing, respect to the gantry zero test plan, a compensation of doses in a symmetric irradiation configuration.

Conclusion

The patient could safely be treated regardless of the metallic prosthesis.

P03

Implementation of ISP Gafchromic EBT3 film using commercial software

Angèle Dubouloz

University Hospital, Geneva, Switzerland

Purpose: Investigate ISP Gafchromic EBT3 films for dose IMRT, VMAT and stereotactic treatment verifications due to the forced disuse of conventional films.

Methods and materials: A flatbed RGB scanner (Epson Expression 10000 XL) was used to digitize radio chromic films using ISP's recommendations for film scanning. Resolution of 72 dpi was used except when verifying stereotactic treatments. Newton's Ring pattern which was problematic on EBT2 films was no longer visible on EBT3 films. Home-made cardboard templates were used to place films at the same position on the flatbed scanner. Study of the time-dependence response was made to estimate the best delay between irradiation and scanning. Analyses were performed using RIT 5.3 software. It contains specific features for radio chromic film analyses as dose calibration, flatbed and non-uniformity corrections. These were compared to traditional standard film analysis. PMMA slide phantom was used for conventional and IMRT verifications, Octavius phantom (PTW) for VMAT, Dynamic Thorax Phantom (CIRS) for IMRT and VMAT lung treatments, Lucy 3D QA phantom (Standard imaging) for stereotactic treatments. 2D dose distributions were calculated with Eclipse 10.0 and then exported to RIT. Absolute and relative dose analysis were done for dose levels from 0 to 20 Gy.

Results: The traditional perpendicular dose calibration was more reproducible and flexible in use than the specific radio chromic calibration. Flat-bed correction contained several bugs and could not be achieved. A delay of 24 hours between irradiation and digitalization was selected for both dose stabilization and practical reasons. Two calibration curves were used depending of the maximum attended dose: red component for dose below 10 Gy and green component from 10 to 20 Gy. The 2D relative dose distribution matching was assessed using gamma criteria 3%/3mm except 5%/0.3mm for stereotactic treatments. The passing rate of 95 % was achieved in the majority of relative study. Absolute film dosimetry results were been judged as not clinically useful.

Conclusion: Gafchromic EBT3 film dosimetry using a commercial software was studied. Specific corrections for radiochromic films were not reproducible and only relative dose measurements were found correct, comparable to other measuring methods.

P04

Radiation Transport Through Beam Modifiers for Proton Radiotherapy Using Macro Monte Carlo

M. K. Fix, D. Frei, W. Volken, E.J. Born, D.M. Aebersold, P. Manser

Division of Medical Radiation Physics and Department of Radiation Oncology, Inselspital, Bern University Hospital, and University of Bern, Switzerland

Introduction: Currently most proton treatments are delivered by utilizing blocks and compensators. These beam modifiers are challenging for beam models using pencil beam dose calculation algorithms. Alternatively, instead of pencil beam algorithms, Monte Carlo (MC) methods can be used for dose calculations in patients, e.g. using the previously developed macro MC (MMC) for protons [1]. The aim of this work is to use the MMC also for the radiation transport through the block and compensator.

Materials & Methods: In this work blocks made of brass and compensators made of pmma have been investigated. For this purpose, local simulations, i.e. full MC simulations using Geant, for brass and pmma materials have been performed for slabs of different thicknesses and different mono-energetic proton pencil beams. The radiation transport through the beam modifiers has been tested for two situations: first a simple $5 \times 5 \text{ cm}^2$ squared block has been used together with a compensator of constant thickness of 2 mm. Second a block-compensator combination from a patient treatment field has been used. For these beam modifiers the dose distribution in a water phantom has been calculated for a mono-energetic parallel proton beam of 160 MeV. Different MC transport methods have been used for the calculations: in a first step the proton beam have been transported through the beam modifiers after which a phase space file has been stored using either Geant or MMC as particle transport method. For each of the two phase space files the dose distribution with a resolution of the dose grid of $2 \times 2 \times 1 \text{ mm}^3$ has been calculated in water using again either Geant or MMC leading to a total of 4 different combinations. The corresponding dose distributions have been compared.

Results: The agreement between the corresponding dose distributions calculated using either Geant or MMC is within 1% or 1 mm for both situations investigated in this study. The calculation speed for MMC is between a factor of 100 and 180 faster than Geant depending on the complexity of the compensator.

Conclusions: The very good agreement between the calculated dose distributions suggests that the radiation transport through block and compensator can be performed accurately and efficiently by using MMC.

Conflict of Interest: This work was supported by Varian Medical Systems.

References

[1] M.K. Fix, D. Frei, W. Volken, E.J. Born, D. Aebersold, P. Manser, *Macro Monte Carlo for Proton Dose Calculation in Different Materials*, Med. Phys. 39(6), 3873, 2012.

P05

Linac Radiation Shielding under clinical conditions - Radiation Protection Case Report

Käthy Haller(1), Stephan Scheidegger(2), Gerd Lutters(1)
(1) Institut für Radio-Onkologie, Kantonsspital Aarau, Switzerland
(2) Zurich University of Applied Science, Winterthur, Switzerland

Introduction

Due to operational reasons at KSA, construction-work was necessary within a controlled area. Some preliminary measurements were made under worst-case conditions to estimate the exposure dose of the constructors. It is quite clear that this is an overestimation, but not by how much. The suspicion was that the shielding of the roof is better than expected from radiation protection estimates.

Materials and Methods

At KSA, there are 3 Siemens linear accelerators. Linacs 1 & 2 (18MV available) are in a bunker with higher bunkerwalls compared to the normal roof level and Linac 3 (6MV only) has equal roof level as the rest of the building.

For estimation we measured the doses on the roof coming from the Linacs with the gantry turned to the ceiling or directed at the measurement points (through the edge wall-ceiling). We used a 40cmx40cm-field irradiating a water-barrel of 20 l on the table for scatter. As dosimeters a STEP RGD 27091, STEP OD-01 Hx, identiFINDER-N, and a Nuclear Enterprises NM2 (neutron dosimeter) was used. Based on these measurements, rules were established for irradiation time slots and construction working hours. During construction, the radiation was monitored with two types of dosimeters at the most critical points: “permanent” measurements with TLDs and on-site dosimeters limited to the hours of exposure of the constructors (TLDs and electronic personal dosimeters (Panasonic EPD, ZP-1463AC1 with a lower threshold of 1 μ Sv)). Panasonic TLDs were used with readout by Dosislab AG.

Results

For the preliminary measurements to estimate the dose on the roof during irradiation, at Linacs 1 & 2 dose rates up to 7.5 μ Sv/h (γ and n dose) were observed. The dose rate was significantly higher for 18MV irradiation compared to 6MV. The neutrons were measured for higher energy only. For Linac 3, γ -dose rates of up to 700 μ Sv/h were measured. The decision was to allow access to the roof only under the conditions that Linac 3 was off and 18MV photons were not in use. During the construction-period, the EPDs showed no dose over 1 μ Sv per day. Sometimes the peak dose rate reached the lower threshold. With this the exposure over 15 weeks for construction workers was less than 28 μ Sv. The γ -TLDs did not reach the lower threshold of 75 μ Sv and for the neutrons a max. dose of 74 μ Sv was recorded.

Discussion

Over 15 weeks we measured less than 75 μ Sv photon and 74 μ Sv neutron dose with the permanent dosimeter on the roof at the most critical points. This dose was measured for all irradiations. Summing up the worst case of mixed dose, this gives 10 μ Sv per week. This does not require a controlled area on the roof. There are some reasons why the dose on the roof during “normal” patient-operation could be higher (i.e. higher portion of 18MV-treatments). To make a clear statement, further measurements are needed. Another interesting aspect would be to find factors to convert measured dose rate at worst case conditions to dose during clinical operation.

P06

Evaluation of the RADPAD® Scatter Protection Shielding using an Alderson phantom in a clinical situation (cardiology)

Käthy Haller(1), Barbara Markert(1), Leandro De Abreu Vieira(1), Gerd Lutters(1),
Stephan Scheidegger(2)

(1) Fachstelle Strahlenschutz, Kantonsspital Aarau, Switzerland

(2) Zurich University of Applied Science, Winterthur, Switzerland

Introduction

To reduce the exposure to scattered radiation in cardiology, surgical drapes (e.g. RADPAD) can be used with or without other protective devices such as lead glass panels. Several clinical studies investigating the $H_p(10)$ -values after a number of real interventions have been carried out to evaluate the impact of RADPAD®. Since these values are not representative of the exposure to the eye lenses, thyroid and extremities, additional measurements with dosimeters at such positions should be performed. Studies have also been made with RADPAD® in a clearly defined setup using phantoms, however not comparable to the clinical situation. In this study, we measure the exposure to the cardiologist in a setup with phantoms comparable to the clinical situation.

Materials and Methods

The chosen setup is close to the situation during cardiac surgery with radial entry. The patient is approximated by an Alderson phantom. To represent the cardiologist, a lead apron was hung on an infusion-stand near the right arm of the patient. The dosimeters were placed on the shoulder, in front of the stomach and at the position of the feet and at the hands of the cardiologist during the intervention. For measurements, the Unfors RaySave i2-system and at the feet, a STEP OD-01 Hx were used. The C-arc of the Siemens AXIOM Artis dFC fluoroscopy unit was in a vertical position (tube position below patients table). Open field (no collimation) was used. The dose rate was integrated during a 15s period of irradiation with the fluoroscopy-mode. The measurements were performed without and with RADPAD® at different positions. For each setup, at least 4 measurements were acquired.

Results

For the measurement points on the body-trunk the reduction of dose was 73% ($\pm 7\%$) at the shoulder and 61% ($\pm 6\%$) at the stomach of the cardiologist. These reductions were reached with the RADPAD® out of field, around the patient body with the arm located outside of the drape (on the top of the shielding). At the hand position a reduction of 54% ($\pm 16\%$) was achieved using the drape. At the feet position the effect was smallest: 7.5% ($\pm 2\%$) reduction in dose rate with the STEP dosimeter, with the RaySafe 22% ($\pm 5\%$).

Discussion and Conclusions

The use of a radiation protection surgical drape can clearly reduce scatter radiation to the cardiologist. As expected, the main impact is over the drape. Below the table, the reduction is minimal (but at least there is no increase of scatter). Depending on the measurement point, the biggest reduction of scattered radiation is reached when putting the drape around the patient body including right arm or around the patient body with the arm lying on the top of the drape. The results seem to be in accordance to the findings of older studies, where the personal dose is evaluated after a certain number of interventions. Beside this, the influence of exact positioning and the combined use with other protective panels is unclear. Further investigations are needed.

P07

Comparison of VMAT plans with variable and constant dose rate and gantry speed for pelvic cancer treatment

Nasser Hejira(1), Grégory Bolard(1,2), Shelley Bulling(2)

(1) Clinique de Genolier, Genolier, Switzerland

(2) Centre d'Oncologie des Eaux-Vives, Geneva, Switzerland

Purpose: We performed a comprehensive comparative study of plan quality for volumetric modulated arc therapy (VMAT) plans for pelvis treatment, optimized with and without variable gantry speed and dose rate.

Methods and Materials: Twelve patients with various pelvic cancers were selected for the study. For each patient, two VMAT plans were generated; (1) fixed gantry speed and dose rate (MU/deg constant), and (2) variable gantry speed and dose rate (MU/deg variable). Plans were optimized using the Pinnacle³ SmartArc treatment planning system to achieve the same planning target volume (PTV) coverage (99% of the PTV is covered by at least 95% of the prescribed dose) and using the same optimization parameters for organs at risk (OAR) and avoidance structures. Plan quality for target coverage was evaluated using the conformity index (CI) and heterogeneity index (HI). The dose to rectum, bladder, and femoral heads was evaluated using Equivalent Uniform Dose (EUD). Efficiency was assessed by comparing the total number of monitor units (MU) and treatment delivery time.

Results: We distinguish two classes of PTV, “simple” and “complex”, depending on the shape and volume of the PTV (degree of concavity, separation of volumes on the same anatomical slice). For a “simple” PTV, the introduction of variable MU per degree for the VMAT plan has very little impact on the PTV coverage and OAR dose. For a “complex” PTV, e.g. prostate and pelvic lymph nodes, the variable gantry speed and dose rate plans have significantly better PTV coverage and rectum sparing. Generally, the VMAT plans with MU/deg variable use approximately 10-15% fewer MU than the fixed dose rate/gantry speed plans. The treatment delivery time is around 90 seconds for a SmartArc variable dose rate plan – a reduction of about 20 seconds compared to MU/deg constant plans.

Conclusion: For simple pelvic PTVs, the plan quality (PTV coverage, OAR EUD) is the same for fixed and variable gantry speed/dose rate plans, but variable plans use fewer MU. For complex pelvic target volumes, variable gantry speed and dose rate plans are superior for both PTV coverage and OAR dose.

P08

Film dosimetry with ImageMagick

Götz Kohle(1), Leandro De Abreu Vieira(1,2)

(1) Klinik für Strahlentherapie und Radioonkologie, Universitätsspital Basel, Switzerland

(2) Kantonsspital Aarau, Radiation-Protection Department, Switzerland

Film dosimetry is part of the quality assurance program in many institutions with radiotherapeutics. The easy handling as well as the high two dimensional spatial resolution are great advantages of film dosimetry. Formerly, film analysis was done by densitometers point by point, whereas nowadays the usage of scanners is the standard. After the scanning process the images has to be analyzed by image processing to convert scanner response to dose. Even if a number of commercial software exists to perform high quality image processing, it is still usually in many institutions to use self-made software solutions.

In our institution most of the EPID (electronic portal image devices) based linac quality assurance tools are implemented using ImageMagick (Kohler G, Linac QS mit ImageMagick; DreiLändertagung 2011, poster). Recently, we have also established a film dosimetry procedure written as ImageMagick script.

ImageMagick is a software suite which initial intend is to process real images. The great power of ImageMagick is the usage on the command line. A lot of procedures can be realized with short commands or scripts on a Unix/Linux shell or on the Windows command line. Even if the mathematical capabilities of ImageMagick are limited it is possible to perform high quality data processing. Another big advantage of ImageMagick is its availability for almost all operating systems as free software delivered as a ready-to-run binary distribution or as source code that you may freely use, copy, modify, and distribute in both open and proprietary applications. It is part of most of the Linux live distributions and thus can be used without installing any software on your computer.

The core of our film dosimetry implementation is written with a few lines of script code. Our poster presentation will be an introduction and a guide line how to implement film dosimetry with ImageMagick. All necessary script lines are included as a ready to go introduction with explanations. For the usage with the EBT 2/3 Gafchromic films color channel separation as well as the blue channel correction method is included. The script lines for the scanner response to dose conversion are shown with different methods. It is shown how easy isodose lines can be drawn in various colors within a single command. This simple script code can be used as a stand-alone solution or as a secondary method to check the primary used method.

For the future we are going to improve our implementation by including the three channel correction method as well as the gamma criterion in our scripts.

P09

Penetration depth of heat produced by superficial hyperthermia applicator in a muscle equivalent phantom material at different surface cooling temperatures

Dietmar Marder

Institut für Radio-Onkologie, Kantonsspital Aarau, Switzerland

Objective: The BSD 500 system is used to treat superficial tumours with hyperthermia (to temperatures of 41-43°C) and is used in combination with radiotherapy. The heat distribution induced by a superficial hyperthermia applicator was studied at various depths in a muscle equivalent phantom. The effect of different surface cooling temperatures was investigated and the results and implications for patient treatment are presented.

Materials and Methods: A muscle equivalent mixture, with a composition as described in literature made from 60% saline (2% NaCl per l) 22.5% sugar and 17.5% super stuff (TX-150), was filled into an acrylic outer casing. Catheters, designed to hold temperature sensors, are positioned on the surface and at three depths within the phantom at 1 cm separation. After heating the phantom material using an 8-Spiral antenna applicator, temperature curves were recorded at 0-3 cm depth. Whilst varying the temperature of an additional surface cooling water bolus, the behaviour of the temperature at depth was measured repeatedly.

Results: A variation in temperature of 4°C for the surface cooling water bolus leads to an increased temperature of 2°C at a depth of 1cm. Generally an increased heat pattern in the depth was produced by decreasing the cooling water temperature. A graphical representation of the depth profiles show that the maximum temperature can not be placed deeper than 2 cm in the phantom material.

Conclusion: The measurements show an upper limit for the deposit of heat in tissue equivalent material using superficial hyperthermia. Since no heat transport due to blood flow was present in the phantom the actual temperatures in human muscle tissue will be lower. Surface cooling can be used to increase temperature at depth but interstitial temperature measurement will be necessary for monitoring in patient treatment.

P10

Development of Scatter Correction Methods for Micro Cone Beam Computed Tomography

W. Volken(1), M. K. Fix(1), D. Frei(1), M. A. Zulliger(2), P. Manser(1)

(1) Division of Medical Radiation Physics and Department of Radiation Oncology, Inselspital, Bern University Hospital, and University of Bern, Switzerland

(2) SCANCO Medical AG, Brüttisellen, Switzerland

Introduction: Micro CBCT scanners have a broad spectrum of applications, e.g. in medicine and material science. However, CBCT suffers from scatter radiation and spectral effects such as beam hardening (BH). Precision of material quantities such as local bone mineral density therefore suffers. In this work an iterative BH- and scatter-correction algorithm was developed by using Monte Carlo (MC) methods.

Materials & Methods: Two micro CBCT scanner models (XtremeCT and μ CT100 from SCANCO Medical AG) were simulated and validated using the EGSnrc/EGS++ MC framework resulting in a virtual scanner model. By separating and analyzing the detector response of direct and scattered particles, fundamental quantities were derived which are suitable for the development of an iterative correction algorithm. This algorithm works as follows: In a first step, the projections measured by the scanner are reconstructed by the system's standard reconstruction algorithm. The reconstructed linear attenuation coefficients are mapped to predefined materials and the resulting phantom is fed into the virtual scanner model where direct and scattered detector signals are calculated analytically using single scatter approximation. For each projection, correction factors are determined to compensate scattered particles and spectral effects. These correction factors are applied to the initially measured projections and reconstructed again, resulting in a better estimate of the scanned object for the next iteration step.

Results: The iterative correction algorithm was tested extensively with different geometrical phantoms and a high resolution XtremeCT tibia scan. For the geometrical phantoms whose material composition is known, the reconstructed linear attenuation coefficients converge to the mono-energetic reference values after 2-3 iteration steps with a deviation of about 1%. For a tibia scan, differences up to 12% compared to the standard correction algorithm were observed in the high-density cortical regions.

Conclusions: The developed iterative correction algorithm for scatter and spectral effects using single scatter approximation presented in this work is a feasible and accurate method to correct micro CBCT data in a consistent and robust way applying basic physics principles without using an extensive pre-calculated scatter kernel database or sophisticated object size estimation models.

Conflict of Interest: This work was supported by the CTI (Project-No. 10629.1) and SCANCO Medical AG.

P11

Qualitative assessment of radiation protection behavior of interventional radiology/cardiology staff using active dosimetry

Nick Ryckx(1), Francis R. Verdun(1), Marta Sans-Mercede(1,2), Jean-Christophe Stauffer(3,4), Alban Denys(3), Yann Lachezal(3), Olivier Muller(3)

(1) Institute of Radiation Physics, Lausanne, Switzerland

(2) Geneva University Hospital, Geneva, Switzerland

(3) Lausanne University Hospital, Lausanne, Switzerland

(4) Fribourg Hospital, Fribourg, Switzerland

The multiplication of lowly-invasive diagnostic and therapeutic procedures using fluoroscopic imaging modalities leads to an increase of scattered X-ray radiation to the medical staff. In this scope, added to a near-future decrease of legal dose limits (especially to the eye lens), there is a strong need to determine if the staff involved in that kind of procedures correctly applies the precepts of radiation protection. Recently, Philips Healthcare (the Netherlands) developed a new system called DoseAware. It consists of active personal dosimeters (PDMs) connected to a base station via radiofrequency. That station, mounted next to the displays in the interventional radiology/cardiology (IR/IC) room, has a screen that graphically shows the respective dose rates of the staff equipped with the PDMs. The system also allows for an immediate visualization of the cumulated dose and average and peak dose rates of every individual PDM. This can be used for self-assessment by the staff during their daily routine or by the medical physicists in the framework of the application of article 74 of the ordinance on radiation protection (StSV/ORaP). Staff has been monitored this way in IR/IC rooms at the Lausanne University Hospital (CHUV) and Fribourg Hospital (HFR) in Switzerland. Furthermore, several parameters such as DAP, air kerma, scopy time, cumulated staff dose and average and peak dose rates were systematically collected after each case. Those parameters permitted the evaluation of the complexity of the intervention and to make the dosimetric results comparable. In addition, several interventions have been video-recorded.

The collected data allowed for a case-by-case awareness of the parameters that have an impact on the instantaneous dose rates and cumulated doses, such as image acquisition frequency, tube orientation, use of collimation, patient thickness, as well as the staff distance to the tube or use/misuse of the protective screens placed around the patient and on the operation table. In addition, it also helped pointing out whether or not the people not directly next to the table were positioning themselves correctly with respect to the tube or, when there was a need for physical proximity with the patient, the operator did not take the staff member's presence into account. Among the results, it has been often noted that a staff member who needed to inject medication in a central line when the operator was scoping at the same time ended the intervention with higher dose/dose rate values than those of the main operator, even if his/her exposure time was significantly lower.

In conclusion, we can say that the DoseAware system allowed the interventionists and the staff of IR/IC rooms to increase their own risk awareness regarding scattered radiation. By displaying the respective dose rates, it allowed them to realize which operational parameters tend to increase the respective dose rates of the people in the IR/IC room. The DoseAware system proves a valuable tool to assess the compliance with respect to the radiation protection norms, be it internally (self-assessment) or externally (medical physicist).